mathematics

MDPI

Article

Nonlinear Smooth Sliding Mode Control Framework for a Tumor-Immune Dynamical System Under Combined Radio-Chemotherapy

Muhammad Arsalan [1], Sadiq Muhammad [2,*] and Muhammad Tariq Sadiq [3,*]

[1] School of Automation, Northwestern Polytechnical University, Xi'an 710072, China; m_arsalan@mail.nwpu.edu.cn
[2] School of Computing, Gachon University, Seongnam-si 13120, Republic of Korea
[3] School of Computer Science and Electronic Engineering, University of Essex, Wivenhoe Park, Colchester CO4 3SQ, UK
* Correspondence: tariqfast@gachon.ac.kr (S.M.); m.t.sadiq@essex.ac.uk (M.T.S.)

Abstract

Sliding mode control (SMC) is a robust nonlinear control framework that enforces system trajectories onto predefined manifolds, providing strong robustness guarantees against uncertainties. However, SMC inherently introduces unwanted transients or chattering in system state trajectories, which may cause issues especially for sensitive applications such as regulation of drug administration. This paper proposes a multi-input smooth sliding mode control (MISSMC) strategy that combines radiotherapy and chemotherapy for a nonlinear tumor–immune dynamical system described by ordinary differential equations. The closed-loop system is first analyzed to establish key qualitative properties: all state variables remain positive and bounded, the sliding surfaces exhibit asymptotic convergence, and explicit analytical upper bounds on the cumulative therapy doses are derived under clinically motivated constraints. On this basis, a smooth hyperbolic-tangent sliding manifold and associated control law are designed to regulate the radiation and drug infusion rates. While the use of a hyperbolic-tangent smoothing function effectively suppresses chattering, it introduces a small steady-state error due to the presence of a boundary layer. To address this limitation, integral action is incorporated into the sliding surfaces, ensuring asymptotic convergence of tumor state and reducing residual steady-state error, while enhancing robustness against model uncertainties and parameter variations. Numerical simulations, based on a brain-tumor case study, show that the proposed smooth SMC markedly suppresses transient overshoots in both states and control inputs, while preserving effective tumor reduction. Compared with a conventional (non-smooth) SMC scheme, the MISSMC controller reduces baseline radiation and chemotherapy intensities on average by roughly 70%. Similarly, MISSMC lowers the overall cumulative doses on average by about 40%, without degrading the therapeutic outcome. The resulting integral smooth SMC framework therefore offers a rigorous nonlinear-systems approach to designing combined radio-chemotherapy protocols with guaranteed positivity, boundedness, and asymptotic stabilization of the closed-loop system, together with explicit bounds on the control inputs.

Keywords: nonlinear dynamical systems; sliding mode control; finite-time stability; Lyapunov analysis; radiotherapy; chemotherapy; tumor–immune model

MSC: 37N25; 93C10; 93D15

Academic Editors: Gualberto Solís-Perales and Adriana Aguilera-González

Received: 22 December 2025
Revised: 19 January 2026
Accepted: 24 January 2026
Published: 1 February 2026

1. Introduction

Tumors arise from the uncontrolled proliferation of abnormal cells that aggregate to form unhealthy lumps and growths [1]. Approximately one in six deaths worldwide is attributed to both direct and indirect causes associated with numerous types of tumors [2,3]. Early diagnosis and swift initiation of treatment procedures greatly enhance the survival rates and, in certain cases, may facilitate remission of this lethal condition [4,5]. In clinical practice, a comprehensive and structured treatment strategy that integrates multiple modalities is commonly employed to mitigate tumor [6]. The choice of treatment procedure is determined by factors including tumor type, grade and other patient-related physical and physiological considerations [7,8]. The following therapeutic approaches are generally considered to manage and treat tumors:

- First-Line Treatment: High-grade tumors, which are characterized by immature, disorganized and rapidly proliferating abnormal cells, are typically treated with surgical resection, followed by concurrent radiotherapy and temozolomide (TMZ)-based chemotherapy. For the treatment of low-grade tumors, post-surgical monitoring is conducted, and depending on tumor progression, delayed radiation or chemotherapy-based intervention, as outlined in the Stupp protocol, may be administered [9,10]. Radiotherapy is generally more localized and may cause comparatively less systemic toxicity than chemotherapy, as chemotherapeutic agents travel through blood stream and are thus more harmful for the human body, but are more effective for malignant tumors [6,11].
- Second-Line Treatment: On the account of failure of first-line treatment, a vascular endothelial growth factor inhibitor Bevacizumab is administered, often in combination with chemotherapy or radiation to treat recurring tumors [12]. Similarly, recent anti-tumor approaches also utilize immune checkpoint inhibitors concurrently with radiation to mitigate tumors effectively [13]. Additionally, patients may be enrolled in clinical trials and other experimental treatments aimed at combating the dynamic adaptability of tumors [7,8,14–16].

  At present, the high-grade tumors are typically treated with surgical resection, followed by concurrent action of radiation therapy and chemotherapy [9,10]. Radiotherapy is generally more localized and may cause comparatively less systemic toxicity than chemotherapy, as chemotherapeutic agents travel through the blood stream and are thus more harmful for the human body, but are more effective for malignant tumors [6,11]. On the account of failure of this first-line treatment, other options such as administration of growth factor inhibitors in combination with chemo-radiotherapy are employed [12,14,15,17].
- Conventional Fixed-Dose Treatment Framework: These therapeutic protocols typically follow a linearly (protocol-based) structured regimen that treats tumors by administering fixed drug dosages at predetermined intervals. These dosages are then adjusted based on regular clinical assessments to evaluate treatment efficacy. Additionally, magnetic resonance imaging (MRI) scans are routinely performed every two to three months to assess disease progression and detect potential recurrence of tumor [6,17,18].

Thus, by applying two or more anti-tumor therapies concurrently, tumor suppression can be enhanced while improving patient outcomes [10,11,16]. However, these multi-modal treatment strategies are associated with significant side effects, as they involve high dosages of radiation or cyto-toxic drugs that not only target cancerous cells but also cause damage to healthy cells. Similarly, these therapies compromise the body's natural immune response against cancer, thus further complicating disease management. Therefore, it is crucial to

develop advanced strategies to regulate drug dosages and prevent excessive radiation exposure, so that patient safety and well-being may be prioritized [19].

Executing experimental research in the domain of tumor management through feedback control is inherently resource-exhaustive and time-consuming [20,21]. Consequently, extensive studies have been conducted to develop mathematical models to study tumor dynamics and predict disease progression, so that feedback control systems maybe designed based on them [22]. The fundamental Gompertzian model provides a foundational framework that describes the influence of chemotherapeutic agents on tumor growth and disease progression [23]. As stated earlier, the anti-tumor drugs are not only detrimental for abnormal tumorous cells, but they also have adverse effects on both healthy as well as immune cells. This harmful impact of chemotherapeutic agents on healthy and tumorous cells has been analyzed recently in the form of a three state model [23,24]. Similarly, the dynamics of the immune system have also been considered to exhibit a more natural and realistic system response [1,3,22,25]. This tumor-immune system model has been further updated to assimilate the dynamics of radiation therapy on tumor progression [11]. However, it is pertinent to highlight that this natural capability of the human immune system to contain the spread of cancerous tumor is not appropriate enough to eliminate it [8,26]. Thus, owing to the complex nonlinear nature of the system, development of novel control strategies for tumor reduction and integration of numerous anti-tumor therapies is of utmost significance.

To coordinate multi-modal therapies, such as chemotherapy, immuno-therapy and radiotherapy, recent clinical studies exploit the tumor micro-environment (TME). Ref. [27] demonstrate TME-responsive nano-platforms for synergistic multi-modal therapy, whereas Ref. [28] illustrates that immuno-modulatory TME frameworks can be utilized beyond oncology to treat inflammatory diseases. Though working at the nano-scale, the outcomes of these studies manifest macroscopic changes in tumor burden, immune response and healthy tissue preservation. ODE-based tumor models provide a complementary, population-level abstraction of these mechanisms, enabling systematic analysis, safety guarantees and feedback-based dosage regulation. The present work leverages that this is clinically inspired while remaining mathematically tractable. From a nonlinear dynamical systems perspective, the tumor-immune-therapy interaction forms a high-dimensional nonlinear ODE system with strong coupling between states and inputs. Understanding its qualitative properties (positivity, boundedness and convergence) and designing robust controllers with asymptotic convergence is therefore of central interest. This work contributes to the analysis and control of such complex dynamical phenomena in a biomedical context.

Recently, various control algorithms and strategies have been proposed to inhibit tumor growth [2,29,30]. Nonlinear control algorithms are the obvious preferred approach to mitigate cancerous tumor, and to halt its proliferation using complex nonlinear system dynamics. Refs. [2,25,31–33] proposed synergetic, state-feedback, sliding mode controller (SMC) and supertwisting algorithms to curb the menace of tumor advancement through chemotherapeutic drug regulation using these nonlinear feedback controllers. Similarly, different variants of nonlinear fuzzy logic-based controllers (FLBCs) have been proposed in Refs. [3,25,30] to manage chemo dosage for tumor mitigation. To fulfill numerous realistic constraints affiliated with the complex process of chemotherapy, optimal control-based controllers have also been proposed [23,24,26,34]. However, the majority of these optimization-based controllers utilize linearized system dynamics, which limit their effectiveness and even result in non-realistic dosage evaluations [11]. A major concern with all of these recently proposed algorithms is the occurrence of highly undesirable transients in control inputs and system states [23,25] as such transients have dire consequences in realistic clinical scenarios [2]. Similarly, tumors are heterogeneous in nature and they

may transform (or develop resistance). Thus, it is pertinent to devise control strategies that consider such model uncertainties and parameter variations into account by utilizing feedback-based regulation to keep tumor cell population and other system states in check.

This research work utilizes an enhanced tumor-immune system interaction model that considers the simultaneous impact of radiotherapy and chemotherapy on tumorous, healthy, and immune cells, to propose a novel multi-input smooth SMC (MISSMC). As discussed above, in order to compensate for any such parameter variations and to mitigate or reduce the steady-state errors caused due to such practical reasons, the proposed algorithm is further upgraded by incorporating integral action within its framework. Several Lyapunov-based and SMC-based controllers have been proposed by employing chemotherapy as a treatment procedure. Yet, these approaches typically neglect the explicit dynamics of radiation. Moreover, they do not guarantee the positivity and boundedness of all states and lack analytical bounds on control inputs or treatment dosages. This research work comprehensively addresses these gaps. The proposed algorithm integrates conventional SMC with a hyperbolic-tangent smoothing function to diminish the transients generated by the nonlinear controller while mitigating the tumor cell population. Similarly, any occurrence or accumulation of steady-state errors within the system is reduced and taken care by the integral action of multi-input integral smooth sliding mode control (MIIS-SMC). Furthermore, by combining both therapies, the proposed treatment strategy aims to limit chemotherapy-related toxicity while efficiently subjugating the cancerous tumor by relying on radiation therapy. Thus, the proposed control mechanism is able to provide a safer and less toxic approach that prioritizes patient health and well-being above all.

The main contributions of this research can be summarized as follows:

1. A multi-input smooth sliding mode controller is developed for a nonlinear tumor-immune model with both radiotherapy and chemotherapy inputs, in which a smooth hyperbolic-tangent function is embedded into the sliding manifold to reduce chattering and undesirable transients.
2. Up-gradation of proposed MISSMC by incorporating integral action within its framework to eliminate residual steady-state errors, while enhancing robustness against model uncertainties and parameter variations.
3. A rigorous analysis of the closed-loop tumor-immune dynamical system is carried out, proving positivity, boundedness and uniform ultimate boundedness of all state variables within a forward-invariant compact set.
4. Using Lyapunov methods, asymptotic convergence of the sliding surfaces is established, together with a corollary that guarantees convergence of the tumor and healthy cell states to their desired equilibrium values.
5. An analytical dosage-bound theorem is derived that provides explicit upper bounds on the cumulative radiation and chemotherapeutic drug doses under prescribed safety constraints.
6. Numerical simulations on tumor case study demonstrate that the proposed MISSMC and MIIS-SMC schemes significantly suppresses transient overshoots and achieves large reductions in both baseline and overall cumulative radiation and drug dosages, while maintaining the desired therapeutic effect, when compared with a conventional (non-smooth) SMC controller.

2. Materials

This research work utilizes a nonlinear mathematical model-based framework to develop a robust, smooth and multi-input SMC for the mitigation of cancerous tumor by regulating combined radiation and chemotherapeutic drug dosage. This section highlights the parameters and variables of considered system model and designed controller. More-

over, the section also provides the research objectives, which serve as the foundation for the development of the control methodology.

2.1. Mathematical Framework

The tumor dynamics model considered in this research study, formulated using ordinary differential equations (ODEs), captures the complex interactions between various cell populations and administered treatment dosages of radiation and chemotherapeutic drugs. The system considers the following state variables:

- T: denotes tumor cell population that proliferate uncontrollably.
- N: denotes normal healthy cells that are directly affected by the treatment.
- I: denotes immune cells that attack tumor cells and are also affected by chemotherapy.
- R: numerically indicates the accumulation of radiation in the body throughout therapy.
- C: numerically indicates the level or presence of chemotherapeutic drug within body during chemotherapy.

The two control inputs which regulate the chemotherapeutic drug and radiation during the combined therapy are as follows:

1. α: the radiation dosage to be administered, computed by the proposed feedback nonlinear controller to curb the progression of cancerous tumor.
2. q: The amount of chemotherapeutic drug to be administered by the proposed feedback nonlinear controller to inhibit tumor growth and mitigate tumor cell population.

A mathematical model based on the ODEs will describe the intricate nonlinear relationships among the system variables, while also incorporating the combined effect of radiation therapy and chemotherapy on the states. The proposed nonlinear smooth SMC is then designed based on this system framework to ensure effective suppression of tumor cells, and thus indirect growth and sustainability of healthy cells.

2.2. Incorporated Dynamics

The following dynamics are considered to provide a comprehensive understanding of the system:

- Healthy and cancerous cells: The system model considers the dynamics of both cancerous and healthy cells to directly exhibit the impact of treatment therapies and immune system response to tumor proliferation as well as their consequences on normal healthy cells.
- Immune system dynamics: To assess the role of the human body's natural resistance to tumor growth and disease advancement, immune cell dynamics have been incorporated.
- Combined radiation and chemotherapy: The system incorporates detailed dynamics of radio-chemotherapy and their combined influence on tumor, healthy and immune cell dynamics.

In this study, radiotherapy and chemotherapy are modeled as continuous control inputs representing average dose rates. The extension to fractionated or bolus-based delivery using impulsive or hybrid control formulations is left for future work

2.3. System Parameters

Apart from system variables, the tumor-immune system dynamical model utilizes a number of parameters that are essential to describe the functioning of system states. These parameters are normalized or scaled (as mentioned in Refs. [1,2,35]), and are pivotal to accurately simulate the disease. These parameters are given below:

- Cell growth rates:

1. r_1: Growth rate of T (tumor cells).
2. r_2: Growth rate of N (healthy cells).
3. r_3: Recruitment rate of I (immune cells).

- Rates of elimination:
  1. a_{12}: Rate of elimination of T by N.
  2. a_{13}: Rate of killing of T by I.
  3. a_{21}: Rate of killing of N by T.
  4. a_{31}: Rate at which T weakens I.
- Drug and Radiation Impacts:
  1. N_T: Proportion representing elimination of T through chemotherapy.
  2. N_N: Proportion representing destruction of N through chemotherapeutic toxicity.
  3. N_I: Proportion of I affected by chemotherapeutic toxicity.
  4. ϵ: Proportion of N affected by radiation-related toxicity.
- Rates of Decay:
  1. Decay rates:
  2. γ: Rate of decay of chemotherapeutic drug.
  3. σ: Rate of decay of radiation.

All these parameters influence the behavior of the system and ensure accurate simulation of treatment procedure.

2.4. Objectives

The main objectives of this research study are as follows:

1. Effective tumor reduction: Achieving a substantial decrease in tumor cell population through a synchronized multi-treatment approach.
2. Reduced side effects: Diminishing the harmful effects of tumor mitigation therapies by lowering the dosages of treatment.
3. Enhanced treatment effectiveness: Decreasing the dosage intensities of combined radio-chemotherapy while ensuring the intended therapeutic results.

By achieving these goals, the proposed methodology aims to enhance patient health outcomes while ensuring the safety and effectiveness of brain tumor therapy.

3. Methods

This section offers a comprehensive explanation of the proposed methodology, derivation of control law and the overall simulation setup. The suggested approach seeks to fulfill the study's goals by integrating a novel nonlinear SMC with effective strategies so that the combined radiation and chemotherapy may be administered with ease and safety.

3.1. Dynamical Nonlinear Model and System Parameters

Most of the ongoing studies focus on regulating the dosage of chemotherapeutic drug without integrating radiation therapy for tumor mitigation. However, as mentioned in Stupp protocol, the combined therapy is more effective [9,10]. The proposed approach not only suggests the combination of both radiation and chemotherapy but it also incorporates hyperbolic-tangent function-based smooth control with the nonlinear MISSMC to ensure smooth and efficient mitigation of cancerous tumor. This control approach is developed using the revised brain tumor dynamics outlines in Equation (1). The considered model builds upon the dynamics introduced in Refs. [1,3,22], incorporating both radiation and chemotherapeutic drug dosages as control inputs.

$$\begin{cases} \dot{T} = r_1 T(1 - \frac{T}{k_1}) - a_{12} NT - a_{13} TI - N_T(1 - e^{-C})T - RT \\ \dot{N} = r_2 N(1 - \frac{N}{k_2}) - a_{21} NT - N_N(1 - e^{-C})N - \epsilon RN \\ \dot{I} = \frac{r_3 IT}{T + k_3} - a_{31} IT - d_3 I - N_I(1 - e^{-C})I \\ \dot{R} = -\gamma R + \alpha \\ \dot{C} = -\sigma C + q \end{cases} \tag{1}$$

The ODE-based dynamical equations exhibited in Equation (1) employ normalized parameters, suggested in Refs. [11,24,25,30,36]. The system presented by Equation (1) is locally Lipchitz on $\mathbb{R}^5_{\geq 0}$. Thus, it exhibits a unique maximal solution for each non-negative initial condition. The adopted tumor-immune system model represents a phenomenological, population-level description of tumor growth and treatment response, capturing the aggregate effects of radiation therapy and chemotherapy, rather than their underlying molecular or cellular mechanisms. Brief explanations of the considered parameters and their respective measurement units are given below:

- Intrinsic growth rate of T: $r_1 = 1.5$ day^{-1};
- Intrinsic growth rate of N:$r_2 = 1$ day^{-1};
- Recruitment rate of I: $r_3 = 0.01$ day^{-1};
- Rate of killing of T by N: $a_{12} = 1$ cells^{-1}day^{-1} ;
- Rate of killing of T by I: $a_{13} = 0.5$ cells^{-1}day^{-1};
- Rate of killing of N by T: $a_{21} = 1$ cells^{-1}day^{-1};
- Rate of killing of I by T: $a_{31} = 1$ cells^{-1}day^{-1};
- Proportion of T eliminated by Chemo: $N_T = 0.5$ day^{-1};
- Proportion of N eliminated by Chemo: $N_N = 0.1$ day^{-1};
- Proportion of I eliminated by Chemo: $N_I = 0.2$ day^{-1};
- Fraction of N killed by radiation: $\epsilon = 0.0008$;
- Natural death rate of I: $d_3 = 0.2$;
- Carrying capacity of T: $k_1 = 1$ cells^{-1};
- Carrying capacity of N: $k_2 = 1$ cells^{-1};
- Carrying capacity of I: $k_3 = 0.3$ cells^2;
- Decaying rate of Radiation: $\gamma = 0.082$ day^{-1};
- Decaying rate of Chemo drug: $\sigma = 0.9$ day^{-1}.

In this study, these model parameters are assumed constant over the considered treatment horizon, reflecting average tumor behavior. In Equation (1), tumor, healthy and immune cells are denoted by "T", "N" and "I", respectively. The amount of radiation inside the considered system is denoted by "R", which is controlled by the administered radiation given α. Similarly, the amount of chemotherapeutic drug within the system is denoted by "C" and it is controlled by the control input q. Hence, the proposed controller will regulate the control inputs, α and q, smoothly to mitigate tumor cell population, and, by doing so, the proposed approach will indirectly stabilize the state representing normal cell population.

The tumor-immune dynamics adopted in Equation (1) represent a control-oriented mathematical model that captures the dominant interactions among tumor cells, healthy cells, immune response, radiotherapy, and chemotherapy, while maintaining analytical tractability for nonlinear controller synthesis. Compared to the models in Refs. [37–39], the present formulation revises the treatment-related terms to explicitly expose the control inputs, enabling the derivation of bounded and positive feedback laws. In particular, the radiation-induced tumor mitigation is modeled using a linear term, which is commonly

employed in continuous-time and moderate fractionation settings in mathematical oncology and the control literature. Clinically, radiation response is often describe by the Linear-Quadratic (LQ) model, which includes both linear and quadratic dose-dependent cell kill terms and is particularly relevant for hypo-fractionated or high-dose radiation protocols. In this study, the quadratic component is intentionally omitted to avoid introducing additional nonlinearities that would significantly complicate the stability analysis and explicit derivation of dose bounds. Moreover, neglecting the quadratic term yields a conservative approximation that may underestimate radiation efficacy at high doses, thereby favoring safety-oriented controller design.

Accordingly, the proposed model should be interpreted as a simplified but clinically motivated representation suitable for feedback control design rather than a high-fidelity radio-biological predictor. Extending the proposed multi-input smoothing sliding mode control framework to tumor models incorporating full LQ radiation dynamics constitutes an important direction for future investigation.

3.2. Basic Properties of System Model

Two basic foundational properties of the tumor-immune system model presented in Equation (1), i.e., positivity and boundedness, are stated and proved here so that they can be utilized in subsequent analysis.

Assumption 1 (Regularity). *The right hand side (RHS) of the system presented in Equation (1) is locally Lipschitz on $\mathbb{R}^5_{\geq 0}$ for non-negative parameters. Thus, for any non-negative initial condition, there exists a unique maximal solution.*

Lemma 1 (Positivity). *Let $T(0), N(0), I(0), R(0), C(0) \geq 0$ and assume both the control inputs α and q are measurable and satisfy $\alpha(t), q(t) \geq 0$ for all $t \geq 0$. Then, the solution of Equation (1) satisfies*

$$T(0), N(0), I(0), R(0), C(0) \geq 0 \text{ for all } t \geq 0.$$

Proof. Consider each coordinate of Equation (1). Evaluated at $T = 0$, the RHS of $\dot{T}$ becomes

$$r_1 T(1 - \frac{T}{k_1}) - a_{12} NT - a_{13} TI - N_T(1 - e^{-C})T - RT = 0 \tag{2}$$

Hence, the vector field points inward or at a tangent to the non-negative orthant on the boundary T = 0. Similarly, the RHS's $\dot{N}$ evaluated at $N = 0$, $\dot{I}$ evaluated at $I = 0$, $\dot{R}$ evaluated at $R = 0$ and $\dot{C}$ evaluated at $C = 0$ are all non-negative (since α, q and all system parameters are non-negative). By utilizing standard forward-invariance arguments for ODEs on $\mathbb{R}^5_{\geq 0}$ (e.g., Nagumo\inward normal condition), the non-negative orthant is a forward-invariant set for the nonlinear tumor-immune dynamical system, ensuring all biologically meaningful states remain non-negative for all $t > 0$. □

Lemma 2 (Boundedness). *Consider there exists α_{max}, $q_{max} \geq 0$, such that $0 \leq \alpha(t) \leq \alpha_{max}$ and $0 \leq q(t) \leq q_{max}$ for all $t \geq 0$. Then, solutions of Equation (1) are uniformly bounded, i.e., there exist constants B_T, B_N, B_I, B_R, $B_C > 0$, such that for any non-negative initial conditions, $0 \leq T(t) \leq B_T$, $0 \leq N(t) \leq B_N$, $0 \leq I(t) \leq B_I$, $0 \leq R(t) \leq B_R$, $0 \leq C(t) \leq B_C$ for all $t \geq 0$.*

Proof. The boundedness of each coordinate of Equation (1) can be proved separately:

Boundedness of states T, N and I: The dynamics of tumor cells ($\dot{T}$) can be re-written as

$$\dot{T} = r_1 T(1 - \frac{T}{k_1}) - \underbrace{(\text{non-negative terms})}_{\geq 0} \tag{3}$$

Thus,

$$\dot{T} \leq r_1 T(1 - \frac{T}{k_1}) \tag{4}$$

The term $r_1 T(1 - \frac{T}{k_1})$ in Equation (4) depicts a classical logistic growth having an upper bound k_1. Thus, the upper bound on state T is given by

$$0 \leq T(t) \leq k_1 =: T_{max} \tag{5}$$

In exactly the same manner, it can be proved that the upper bounds on states N and I, from the system presented by Equation (1), are given by

$$0 \leq N(t) \leq k_2 =: N_{max} \tag{6}$$

$$0 \leq I(t) \leq k_3 =: I_{max} \tag{7}$$

Boundedness of states R and C: The dynamics of state R presented in Equation (1) can be re-written as

$$\dot{R} = -\gamma R + \alpha(t) \leq -\gamma R + \alpha_{max} \tag{8}$$

where α_{max} describes the maximum allowed radiation dosage for treatment. Thus, the upper bound on state R is given by

$$0 \leq R(t) \leq max(R(0), \frac{\alpha_{max}}{\gamma}) =: R_{max} \tag{9}$$

Similarly, for state C, the upper bound is given by

$$0 \leq C(t) \leq max(C(0), \frac{q_{max}}{\sigma}) =: C_{max} \tag{10}$$

Thus, the solution remains inside the compact box $\Omega := [0, T_{max}] \times [0, N_{max}] \times [0, I_{max}] \times [0, R_{max}] \times [0, C_{max}]$, which is a forward-invariant set, proving that the system is uniformly bounded. Hence, the nonlinear tumor-immune dynamical system is uniformly ultimately bounded for all admissible control inputs $\alpha(t)$ and $q(t)$ satisfying $0 \leq \alpha(t) \leq \alpha_{\max}$ and $0 \leq q(t) \leq q_{\max}$. □

3.3. Proposed Control Methodology

A nonlinear MISSMC algorithm has been formulated, built upon nonlinear tumor-immune system dynamics, to mitigate tumor growth and suppress its proliferation using radiation therapy and chemotherapy concurrently. The designed feedback mechanism, exhibited in Figure 1, utilizes the information of system states to derive a control law that systematically regulates therapeutic inputs, ensuring safe and effective delivery of radiation and chemotherapeutic drug dosages for tumor management. Given the highly nonlinear and coupled nature of tumor-immune dynamics, the adoption of a robust sliding mode-based control strategy is particularly advantageous for achieving reliable performance under modeling uncertainties and external disturbances [1,40]. However, feedback controllers in general and nonlinear controllers in particular tend to compute relatively high initial dosages to curb tumor growth rapidly. Moreover, several control-based tumor

treatment strategies reported in the recent literature administer high cumulative dosages over the treatment horizon, potentially leading to excessive toxicity and adverse side effects [2,11]. Additionally, the inherent robustness of the nonlinear controller, which enables rapid compensation for disturbances and parameter variations, may induce transient oscillations in both system states and control inputs [2,25]. To address these challenges, a smooth hyperbolic-tangent switching function is incorporated into the sliding mode framework to effectively suppress chattering and attenuate transient oscillation.

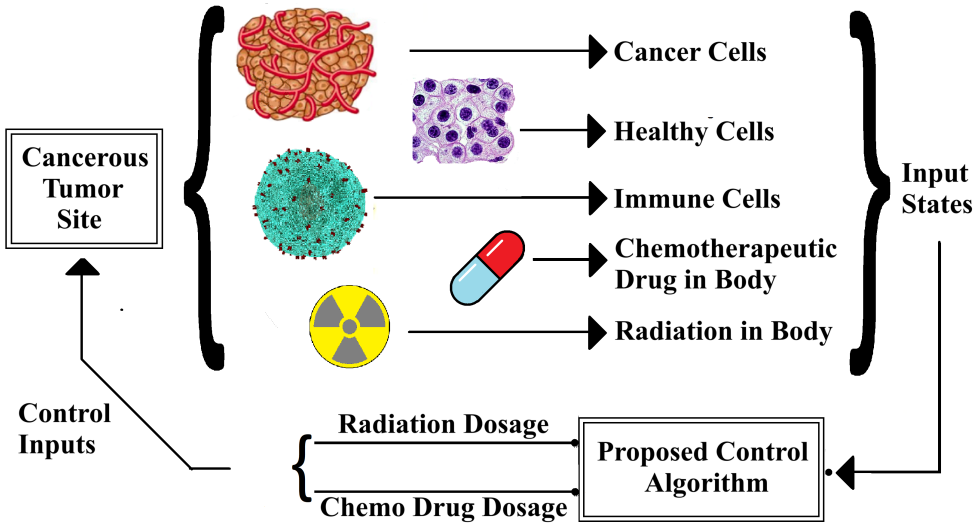

Figure 1. Tumor mitigation using proposed closed-loop methodology.

While the introduction of a smooth switching function significantly improves transient performance, its inevitably gives rise to a boundary layer around the sliding manifold, resulting in a small residual steady-state tracking error. To overcome this limitation, integral action is incorporated into the sliding surfaces associated with tumor and healthy cell dynamics. The resulting multi-input integral smooth sliding mode control (MIIS-SMC) framework accumulates tracking errors over time and actively compensates for boundary-layer-induced offsets, thereby ensuring asymptotic convergence of tumor tracking errors to zero without reintroducing chattering. Furthermore, the inclusion of integral action enhances robustness against parameter variations and model mismatches that may arise due to tumor heterogeneity or long-term therapy effects.

The design process of the MISSMC exploits the impact of radiation therapy and chemotherapy on healthy ("N") and tumor cells ("T"). Accordingly, the control law governing chemotherapeutic drug administration is synthesized primarily based on the tumor cell dynamics, while the radiation dosage control law is derived using the state representing healthy and normal cell population dynamics. This structure enables a coordinated multi-input control strategy in which radio-chemotherapy is applied simultaneously to achieve dual therapeutic objectives: suppressing tumor growth while promoting the recovery and preservation of healthy tissue. The proposed algorithm is designed not only to regulate chemotherapy for reduction of tumor cells, but also to enhance the proliferation of healthy cells by regulating radiation dosages. This dual-objective approach contributes to a more effective and efficient treatment framework. Consequently, the proposed methodology provides a balanced and clinically motivated treatment framework that reduces overall toxicity, mitigates steady-state errors, and prioritizes patient health and well-being while ensuring successful disease alleviation.

3.4. Control Objectives

While the primary objective of the designed control algorithm is to completely eradicate the tumor cell population, several important control objectives that are either directly or indirectly affiliated to the goal of tumor mitigation can be realized:

1. Tumor suppression: Asymptotic regulation of the tumor cell population towards a desired eradication threshold (low-level equilibrium) ($T(t) \leq 10^{-5}$).
2. Preservation of normal healthy cells: Proliferation and perseverance of the normal cell population by avoiding excessive therapeutic intervention.
3. Toxicity reduction: Reduction of cumulative radiation and chemotherapy dosages through a coordinated multi-input control strategy, thereby limiting treatment-related toxicity.
4. Smooth and transient-free application of control action: Suppression of chattering and attenuation of transient oscillations in both system states and control inputs to enhance treatment comfort and safety.
5. Steady-state accuracy and robustness: Elimination of residual steady-state tracking errors, arising from boundary-layer effects or parameter mismatches, through incorporation of integral action with a smooth sliding mode control framework.

3.5. Design of Multi-Input Smooth SMC

The primary objective of the proposed treatment procedure is to subjugate cancerous tumor cells while simultaneously promoting the preservation and proliferation of healthy normal cells. The goal is pursued through the concurrent regulation of radiation and chemotherapeutic drug dosages via the MISSMC approach. The SMC is a distinctive nonlinear control strategy that leverages information from system states to achieve a predefined objective, i.e., the suppression of tumor growth for this research study. Classical SMC yields chattering and large initial control values. To mitigate these effects, a hyperbolic-tangent smoothing function has been employed into a multi-input SMC structure. This function facilitates a gradual adjustment of control inputs, ensuring a more stable and controlled therapeutic response. The proposed feedback process that integrates a smoothing agent with MISSMC is illustrated in Figure 2.

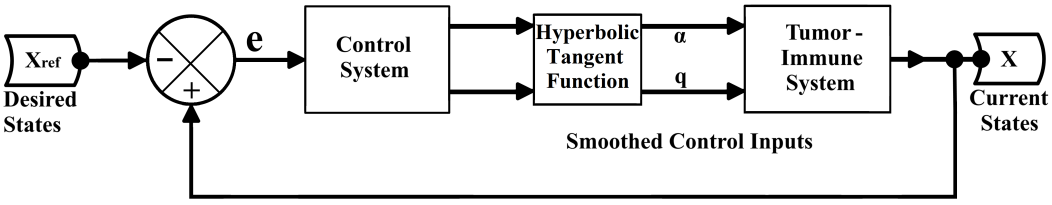

Figure 2. Closed-loop control using multi-input smooth SMC.

Control Law Derivation and Main Stability Theorem

Since the system under consideration utilizes two different control inputs, i.e., radiation and chemotherapeutic drug dosage, two sliding surfaces are considered for each of the considered control inputs, respectively. Let

$$s_T = T - T_d \tag{11}$$

$$s_N = N - N_d \tag{12}$$

where T_d and N_d are the desired or reference values for the states T and N. Moreover, T_d is considered to be 0, as the goal is to reduce the tumor population to 0. Similarly, N_d is

considered to be 1, i.e., the maximum value of normalized healthy cells. As T_d and N_d are constants, the derivatives of the considered sliding surfaces are given by

$$\dot{s}_T = \dot{T} \tag{13}$$

$$\dot{s}_N = \dot{N} \tag{14}$$

To ensure that the system trajectory reaches the considered sliding surfaces and remains confined within them at all times, consider

$$\dot{s}_T = -K_T \times tanh(s_T/\phi_T) \tag{15}$$

$$\dot{s}_N = -K_N \times tanh(s_N/\phi_N) \tag{16}$$

where K_T, K_N, ϕ_T and ϕ_N are the positive-valued design constants. The parameters ϕ_T and ϕ_N determine the steepness of the hyperbolic-tangent function.

The stability of the system can be analyzed by considering the following Lyapunov functions:

$$V_1 = \frac{1}{2}{s_T}^2 \tag{17}$$

$$V_2 = \frac{1}{2}{s_N}^2 \tag{18}$$

By taking the time derivative of Equations (17) and (18), we get

$$\dot{V}_1 = s_T\dot{s}_T = -K_T \times s_T \times tanh(s_T/\phi_T) \tag{19}$$

$$\dot{V}_2 = s_N\dot{s}_N = -K_N \times s_N \times tanh(s_N/\phi_N) \tag{20}$$

Theorem 1 (Asymptotic Convergence of Sliding Surfaces)**.** *Under the assumptions that K_T, K_N, ϕ_T and ϕ_N are positive constants, and that the sliding surface (s_T, s_N) dynamics evolve according to Equations (15) and (16), the sliding variables $s_T(t)$ and $s_N(t)$ converge asymptotically to zero, i.e.,* $\lim_{t\to\infty} s_T(t) = 0, \quad \lim_{t\to\infty} s_N(t) = 0.$

Proof. Consider the Lyapunov function:

$$V(s_T, s_N) = \frac{1}{2}(s_T^2 + s_N^2) \tag{21}$$

which is positive definite and radially unbounded. Taking its time derivative along the closed-loop trajectories yields:

$$\dot{V} = s_T\dot{s}_T + s_N\dot{s}_N = -K_T \times s_T \times \tanh(\frac{s_T}{\phi_T}) - K_N \times s_N \times \tanh(\frac{s_N}{\phi_N}) \tag{22}$$

Since $x\tanh(x/\phi) > 0 \; \forall \; x \neq 0$, it follows that $\dot{V} < 0 \; \forall \; (s_T, s_N) \neq (0,0)$, and $\dot{V} = 0$ if and only if $s_T = s_N = 0$. Therefore, the equilibrium $(s_T, s_N) = (0,0)$ is globally asymptotically stable.

Moreover, using the property $\tanh(z) \leq z$ for $z \geq 0$, it follows that

$$\dot{V} \leq -\frac{K_T}{\phi_T} s_T^2 - \frac{K_N}{\phi_N} s_N^2 \leq -2\min\left(\frac{K_T}{\phi_T}, \frac{K_N}{\phi_N}\right) V \tag{23}$$

Defining $\beta := 2\min\left(\frac{K_T}{\phi_T}, \frac{K_N}{\phi_N}\right) > 0$, we obtain $\dot{V} \leq -\beta V$, which guarantees exponential convergence of the sliding variables to zero. □

Corollary 1 (State Convergence)**.** *By utilizing Theorem 1 and Lemmas 1 and 2 (positivity and boundedness), the closed-loop system states satisfy*

$$\lim_{t\to\infty} T(t) = T_d = 0, \quad \lim_{t\to\infty} N(t) = N_d = 1 \tag{24}$$

Since the reaching law employs a smooth hyperbolic-tangent function, the resulting closed-loop dynamics are locally Lipchitz, which guarantees the existence and uniqueness of solutions, and ensures asymptotic convergence. Finite-time convergence would require a non-smooth reaching law, which is intentionally avoided here to suppress chattering and improve clinical applicability.

Thus, as "K_T" and "K_N" are positive constants, $xtanh(x)$ is always ≥ 0 for all values of x. Hence, the expressions on the right hand side of Equations (19) and (20) remain strictly negative definite in a Lyapunov sense for all values of "s_T" and "s_N", ensuring stability and asymptotic convergence of system trajectories to the considered sliding surfaces.

In order to compute the equations for control laws "α" and "q", the reference value for the states "C" and "R" are required. Thus, by tracking these reference value, the designed controller will be able to administer the appropriate amount of chemotherapeutic drug and radiation dosage. Equations (15) and (16) can be utilized to derive the final expressions for the control laws. Using Equations (1), (13) and (15), we get

$$R = r_1\left(1 - \frac{T}{k_1}\right) - a_{12}N - a_{13}I - N_T\left(1 - e^{-C}\right) + \frac{K_T \times tanh(s_T/\phi_T)}{T} \tag{25}$$

Similarly, another equation for the state variable "R" can be computed using Equations (1), (14) and (16):

$$R = \frac{r_2}{\epsilon}\left(1 - \frac{N}{k_2}\right) - \frac{a_{21}T}{\epsilon} - \frac{N_N}{\epsilon}\left(1 - e^{-C}\right) + \frac{K_N \times tanh(s_N/\phi_N)}{\epsilon N} \tag{26}$$

Equating Equations (25) and (26), and solving for $(1 - e^{-C})$, we get

$$\begin{aligned}\left(1 - e^{-C}\right) &= \frac{-\epsilon\left(r_1\left(1-\frac{T}{k_1}\right) - a_{12}N - a_{13}I + \frac{K_T \times tanh(s_T/\phi_T)}{T}\right)}{N_N + \epsilon N_T} \\ &+ \frac{r_2\left(1-\frac{N}{k_2}\right) - a_{21}T + \frac{K_N \times tanh(s_N/\phi_N)}{N}}{N_N + \epsilon N_T}\end{aligned} \tag{27}$$

For the sake of simplification, let

$$C_1 = r_1\left(1 - \frac{T}{k_1}\right) - a_{12}N - a_{13}I + \frac{K_T \times tanh(s_T/\phi_T)}{T} \tag{28}$$

$$C_2 = r_2\left(1 - \frac{N}{k_2}\right) - a_{21}T + \frac{K_N \times tanh(s_N/\phi_N)}{N} \tag{29}$$

Thus, Equation (27) becomes

$$\left(1 - e^{-C}\right) = \frac{C_2 - \epsilon C_1}{N_N + \epsilon N_T} \tag{30}$$

Let

$$y = (1 - e^{-C}) \tag{31}$$

Solving for "C" using Equation (31)

$$C^* = -ln(1 - y) \tag{32}$$

Here, the "C^*" represents the reference value of chemotherapeutic drug required inside the body to successfully mitigate tumor. Similarly, the reference value for the state "R" can be evaluated by substituting "y" from Equation (31) into Equation (25):

$$R^* = \frac{C_1 N_N - C_2 N_T}{N_N - \epsilon N_T} \tag{33}$$

Now, to force "C" $\rightarrow$ "C^*", let

$$q = \sigma C^* + K_C \times tanh(C - C^*) \tag{34}$$

where "K_C" is a positive design constant. Similarly, to force "R" $\rightarrow$ "R^*", let

$$\alpha = \gamma R^* + K_R \times tanh(R - R^*) \tag{35}$$

where "K_R" is a positive design constant. By administering the control laws provided in Equations (34) and (35), the terms "σC^*" and "γR^*" negate the impact of natural decay terms "$-\sigma C$" and "$-\gamma R$", respectively, when "C" $\rightarrow$ "C^*" and "R" $\rightarrow$ "R^*". Whereas, the switching terms "$K_C \times tanh(C - C^*)$" and "$K_R \times tanh(R - R^*)$" overcome disturbances and drive the states to their respective references robustly. Thus, Equations (34) and (35) ensure robust convergence of system states to their desired references. Moreover, the hyperbolic-tangent terms ensure smooth as well as robust transitions of system states to their final values.

Theorem 2 (Treatment Dosage Bounds)**.** *Consider that Lemma 2 holds and the design constants and parameters satisfy*

$$|C_1(t)| \leq \bar{C}_1, \ |C_2(t)| \leq \bar{C}_2 \text{ for all } t > 0 \tag{36}$$

where $\bar{C}_1$ and $\bar{C}_2$ follow from bounds on T, N, I. If the bounds satisfy

$$0 \leq \underline{y} \leq y(t) \leq \bar{y} < 1 \text{ for all } t, \tag{37}$$

then $C^* = -ln(1 - y)$ satisfies

$$0 \leq C^*(t) \leq -ln(1 - \bar{y}) \tag{38}$$

Therefore, the controller given by Equation (34) ($q(t) = \sigma C^* + K_C \times tanh(C - C^*)$) satisfies

$$0 \leq q(t) \leq \sigma(-ln(1 - \bar{y})) + K_C \tag{39}$$

A similar upper bound holds for $\alpha(t) = \gamma R^* + K_R \times tanh(R - R^*)$. Hence, by choosing design parameters and verifying the numerical values of $\bar{y}$, it can be guaranteed that the controls remain within clinically acceptable bounds, i.e., $0 \leq q(t) \leq q_{max}$, $0 \leq \alpha(t) \leq \alpha_{max}$

Proof. The algorithm computes reference concentrations C^* and R^*, which are computed by algebraic combination of the bounded state-dependent quantities C_1, C_2. By utilizing Lemma 2 to bound state-dependent terms and by ensuring that the denominator (of Equations (30) and (33)) never approaches zero, and the resulting fraction stays in $[0, 1)$, then monotonicity of $-ln(1-*)$ gives an explicit upper bound for C^* (and similarly for R^* as well). Thus, adding the bounded *tanh* terms yields explicit bounds on q and α. Numerical verification in Section 4 demonstrates that the bounds are conservative. □

3.6. Multi-Input-Integral Smooth SMC (MIIS-SMC)

The proposed MISSMC, designed in Section Control Law Derivation and Main Stability Theorem, effectively reduces chattering while offering asymptotic convergence of states. However, the hyperbolic-tangent-based smooth switching function introduces a small steady-state error due to the presence of a boundary layer. Similarly, the system parameters considered by the study (presented in Section 3.1) can vary, especially if the combined therapy continues for a long time. The proposed MISSMC is robust, yet the algorithm is not capable of compensating for such variations. The impact of such parameter uncertainties also results in the accumulation of steady-state errors. By introducing integral action within the framework of a smooth SMC, these accumulated steady-state errors can be drastically reduced without re-introducing chattering. The controller design procedure and main stability theorem provided in Section Control Law Derivation and Main Stability Theorem can be utilized again to introduce integral action in the MISSMC to formulate a multi-input-integral smooth SMC (MIIS-SMC). Consider the following two sliding surfaces:

$$s_{Ti} = s_T(t) + \lambda_T \int_0^t s_T(\tau) d\tau \tag{40}$$

$$s_{Ni} = s_N(t) + \lambda_N \int_0^t s_N(\tau) d\tau \tag{41}$$

where s_T and s_N are given by Equations (11) and (12). The terms $\lambda_T \int_0^t s_T(\tau) d\tau$ and $\lambda_N \int_0^t s_N(\tau) d\tau$ represent the accumulated errors, whereas λ_T and λ_N are positive definite integral gains. The time derivative of s_{Ti} and s_{Ni} will be

$$\dot{s}_{Ti} = \dot{T} + \lambda_T s_T(t) \tag{42}$$

$$\dot{s}_{Ni} = \dot{N} + \lambda_N s_N(t) \tag{43}$$

To ensure that the system trajectory reaches the considered sliding surfaces and remains confined within them at all times, consider

$$\dot{s}_{Ti} = -K_T \times tanh(s_{Ti}/\phi_T) \tag{44}$$

$$\dot{s}_{Ni} = -K_N \times tanh(s_{Ni}/\phi_N) \tag{45}$$

The stability of the system can be analyzed by considering the following Lyapunov functions:

$$V_{1i} = \frac{1}{2} {s_{Ti}}^2 \tag{46}$$

$$V_{2i} = \frac{1}{2}{s_{Ni}}^2 \tag{47}$$

By taking time derivatives of Equations (46) and (47), we get

$$\dot{V}_{1i} = s_{Ti}\dot{s}_{Ti} = -K_T \times s_{Ti} \times tanh(s_{Ti}/\phi_T) \tag{48}$$

$$\dot{V}_{2i} = s_{Ni}\dot{s}_{Ni} = -K_N \times s_{Ni} \times tanh(s_{Ni}/\phi_N) \tag{49}$$

Since the hyperbolic-tangent function satisfies

$$s_x \times tanh(\frac{x}{\phi}) > 0 \; \forall \; s_x \neq 0 \tag{50}$$

it follows that

$$\dot{V}_{1i} \leq 0 \; \forall \; s_{Ti} \neq 0 \tag{51}$$

and

$$\dot{V}_{2i} \leq 0 \; \forall \; s_{Ni} \neq 0 \tag{52}$$

Moreover, $\dot{V}_{1i} = 0$ if and only if $s_{Ti} = 0$ and $\dot{V}_{2i} = 0$ if and only if $s_{Ni} = 0$. Hence, $\dot{V}_{1i}$ and $\dot{V}_{2i}$ are negative definite for all non-zero s_{Ti} and s_{Ni}, implying

$$\lim_{t\to\infty} s_{Ti} = 0 \text{ and } \lim_{t\to\infty} s_{Ni} = 0 \tag{53}$$

Since s_{Ti} (or s_{Ni}) is bounded and converges to zero, and $s_{Ti} = s_T(t) + \lambda_T \int_0^t s_T(\tau)d\tau$, it follows that $s_T(t)$ must converge to zero. Otherwise, the integral term would diverge, contradicting the boundedness of s_{Ti}. Hence, the tumor tracking error converges asymptotically to zero. Now, in order to compute the equations for control laws "α" and "q", the reference values for the states "C" and "R" are required. Using Equations (1), (42) and (44), we get

$$R = r_1(1 - \frac{T}{k_1}) - a_{12}N - a_{13}I - N_T(1 - e^{-C}) + \frac{K_T \times tanh(s_{Ti}/\phi_T)}{T} + \frac{\lambda_T s_{Ti}}{T} \tag{54}$$

Similarly, another equation for the state variable "R" can be computed using Equations (1), (43) and (45):

$$R = \frac{r_2}{\epsilon}(1 - \frac{N}{k_2}) - \frac{a_{21}T}{\epsilon} - \frac{N_N}{\epsilon}(1 - e^{-C}) + \frac{K_N \times tanh(s_{Ni}/\phi_N)}{\epsilon N} + \frac{\lambda_N s_{Ti}}{N} \tag{55}$$

Equating Equations (54) and (55), and solving for $(1 - e^{-C})$, we get

$$\begin{aligned}(1 - e^{-C}) \quad &= \frac{-\epsilon(r_1(1-\frac{T}{k_1}) - a_{12}N - a_{13}I + \frac{K_T \times tanh(s_{Ti}/\phi_T)}{T})}{N_N + \epsilon N_T} \\ &+ \frac{r_2(1-\frac{N}{k_2}) - a_{21}T + \frac{K_N \times tanh(s_{Ni}/\phi_N)}{N}}{N_N + \epsilon N_T}\end{aligned} \tag{56}$$

For the sake of simplification, let

$$C_{1i} = r_1(1 - \frac{T}{k_1}) - a_{12}N - a_{13}I + \frac{K_T \times tanh(s_{Ti}/\phi_T)}{T} \tag{57}$$

$$C_{2i} = r_2(1 - \frac{N}{k_2}) - a_{21}T + \frac{K_N \times tanh(s_{Ni}/\phi_N)}{N} \tag{58}$$

Thus, Equation (56) becomes

$$(1 - e^{-C}) = \frac{C_2 i - \epsilon C_1 i}{N_N + \epsilon N_T} \tag{59}$$

Let

$$y_i = (1 - e^{-C}) \tag{60}$$

Solving for "C" using Equation (60)

$$C_i^* = -ln(1 - y_i) \tag{61}$$

Here, the "C_i^*" represents the reference value of chemotherapeutic drug. The reference value for the state "R" can be evaluated by substituting "y_i" from Equation (60) into Equation (54):

$$R_i^* = \frac{C_{1i}N_N - C_{2i}N_T}{N_N - \epsilon N_T} \tag{62}$$

Now, to force "C" $\rightarrow$ "C_i^*", let

$$q_i = \sigma C_i^* + K_C \times tanh(C - C_i^*) \tag{63}$$

Similarly, to force "R" $\rightarrow$ "R_i^*", let

$$\alpha_i = \gamma R_i^* + K_R \times tanh(R - R_i^*) \tag{64}$$

where "K_C" and "K_R" are positive design constants. By administering the control laws provided in Equations (63) and (64), the terms "σC_i^*" and "γR_i^*" negate the impact of natural decay terms "$-\sigma C$" and "$-\gamma R$", respectively, when "C" $\rightarrow$ "C_i^*" and "R" $\rightarrow$ "R_i^*", whereas the switching terms "$K_C \times tanh(C - C_i^*)$" and "$K_R \times tanh(R - R_i^*)$" overcome disturbances and drive the states to their respective references robustly. Thus, integral action enables rejection of steady-state errors caused by bounded parameter variations and model mismatch, while preserving asymptotic stability of the sliding surfaces. Moreover, Equations (63) and (64) ensure robust convergence of system states to their desired references, whereas the hyperbolic-tangent terms ensure smooth as well as robust transitions of system states to their final values.

4. Simulation and Results

In this section, the effectiveness of the proposed MISSMC mechanism and the capabilities of MIIS-SMC to reduce tracking errors while enhancing robustness against model uncertainties is assessed. The MISSMC and MIIS-SMC are developed based on an ODE framework that characterize tumor dynamics, as outlined in Equation (1).

4.1. Simulation Setup

In order to validate the performance of the designed algorithm, strict initial conditions for the state variables have been selected. These initial conditions are as follows: $[T_0; N_0; I_0; R_0; C_0] = [0.9; 0.5; 0.1; 0; 0]$. According to these conditions, a high tumor cell population, with no initial radiation and chemotherapeutic drug concentrations, has been opted. Similarly, the healthy cell population is also kept relatively low to rigorously assess and analyze the performance of the controller. Furthermore, apart from assessing the performance of the MIIS-SMC algorithm on the initial conditions mentioned above, the proposed algorithm is further evaluated to analyze its robustness against model uncertainties. This is achieved by keeping the initial conditions the same while varying the tumor growth rate parameter "r_1" to observe the variations in transient response and overall state trajectories. However, it is explicitly stated that throughout this particular experiment to analyze MIIS-SMC, the controller has no information of any parameter mismatch.

4.2. Environment

The nonlinear tumor dynamics model provided in Equation (1) as well as the proposed smooth SMC algorithm have been simulated using MATLAB R2016a.

Controller Design Parameters

The controller design parameters introduced in Section 3.5 play a very critical role in shaping the transient and steady-state behavior of the closed-loop system. In this study, the controller gains were selected using a trial-and-error procedure, with primary objective of achieving smooth system responses while satisfying clinically motivated constraints on radiation and drug dosages. The complete set of selected controller gains used for the proposed MISSMC and MIIS-SMC schemes are provided in Table 1.

Table 1. Model parameters and controller gain values used in simulations.

Parameter	Value	Parameter	Value
K_T: Tumor sliding gain	10.55	ϕ_T: Boundary layer width for T	0.3
K_N: Healthy cell sliding gain	0.5	ϕ_N: Boundary layer width for N	0.3
K_R: Radiotherapy tracking gain	1	λ_T: Integral gain	100
K_C: Chemotherapy tracking gain	60	λ_N: Integral gain	2000

Variations in these parameters primarily influence the transient characteristics of the system, including convergence speed and overshoot, while preserving stability. Accordingly, the gains were tuned to suppress excessive transients and ensure smooth administration of the control inputs. It is important to emphasize that, although empirical tuning was employed to identify a feasible gain set, the robustness of the proposed control framework arises from the inherent sliding mode structure and the incorporation of integral action, rather than from precise gain values. Consequently, the closed-loop system maintains stability and tumor suppression performance in the presence of bounded parameter variations and model uncertainties.

4.3. Performance Comparison Framework

To evaluate the performance of the proposed MISSMC algorithm, the following criteria have been opted:

1. Reduction in baseline radiation and chemotherapeutic drug dosage.
2. Faster convergence time of system states to their desired values, especially the convergence of tumor cell population to zero.

3. Reduction in overall administered dosages of radiation and chemotherapeutic drug during the course of combined therapy.

Similarly, the controller performance is also evaluated qualitatively to highlight the following special features of the proposed controller:

1. Smooth application of control inputs and transient-free system response.
2. Toxic impact of treatment procedure on patient health.
3. Convergence of administered control inputs to zero.
4. Therapy types considered for tumor mitigation.
5. Swiftness in decimation of tumor cell population.

4.4. Bench-Marking

Comprehensive comparative analysis between the performance of the proposed MISSMC (and MIIS-SMC) and algorithms presented in recent times is established based on the performance parameters provided in Section 4.3. To validate the superiority of the proposed algorithms, their performance is compared against state-feedback, FLBC, supertwisting and nonlinear synergetic controllers. Similarly, the performance of the twin delayed deep deterministic (TD3) algorithm is also evaluated so that a meaningful comparison may be established between the proposed nonlinear controller and deep reinforcement learning algorithm.

4.5. Results: SMC vs. Tangent Hyperbolic Function-Based Smooth SMC

To demonstrate the effectiveness and superiority of the proposed MISSMC algorithm, its performance is evaluated by comparing it to the conventional SMC. The dynamics of the tumor and healthy cell population under the impact of both the conventional SMC and the proposed MISSMC have been depicted in Figure 3. Figure 3a depicts the dynamics of the tumor cell population under the impact of respected controllers, whereas Figure 3b depicts the trajectories of healthy cell populations. Similarly, the dynamics of the states "R" and "C" for the case of the SMC and proposed smooth SMC have been depicted in Figure 4. Figure 4a depicts the radiation dynamics in the body over time, under the impact of respected controllers, whereas Figure 4b depicts the chemotherapeutic drug concentration over time. For the case of tumor cell population, both the controllers performed almost identically to each other. However, the conventional SMC depicted large transients in the dynamics of the healthy cell population. On the other hand, the dynamics observed when the proposed smooth SMC is examined depict smooth and transient-free trajectory. Similarly, huge transients can be observed in both radiation and chemotherapeutic drug concentration states when the conventional SMC has been utilized. However, once again, the transients observed in the dynamics of "R" and "C" when the proposed smooth SMC has been utilized are negligible or very few in comparison to those detected while using conventional SMC.

As observed in Figure 5, the control inputs administered by both the considered controllers depict stark differences. Figure 5a depicts the radiation dosages computed by the respective controllers, whereas Figure 5b illustrates chemotherapeutic drug administration by the considered algorithms. In the case of the conventional SMC, frequent transients can be observed in the computed dynamics of both radiation ("α") and chemotherapeutic drug ("q") control inputs. By analyzing the control input "q" computed by the conventional SMC, a high initial dosage has been observed, whereas the initial dosage administered by the proposed smooth SMC is relatively lower. Thus, even though such huge transients are observed in the dynamics of system states as well as the computed control inputs, the SMC still achieved almost similar rise-time and settling-time characteristics as to that of the proposed smooth SMC. However, the proposed controller achieved the same results

while utilizing lesser dosages of radiation and chemo drug inputs. This difference in performance between the two compared controllers has critical consequences, as a higher dosage requirement implies higher treatment-induced toxicity and more risk for the patient under consideration when the conventional SMC is to be utilized.

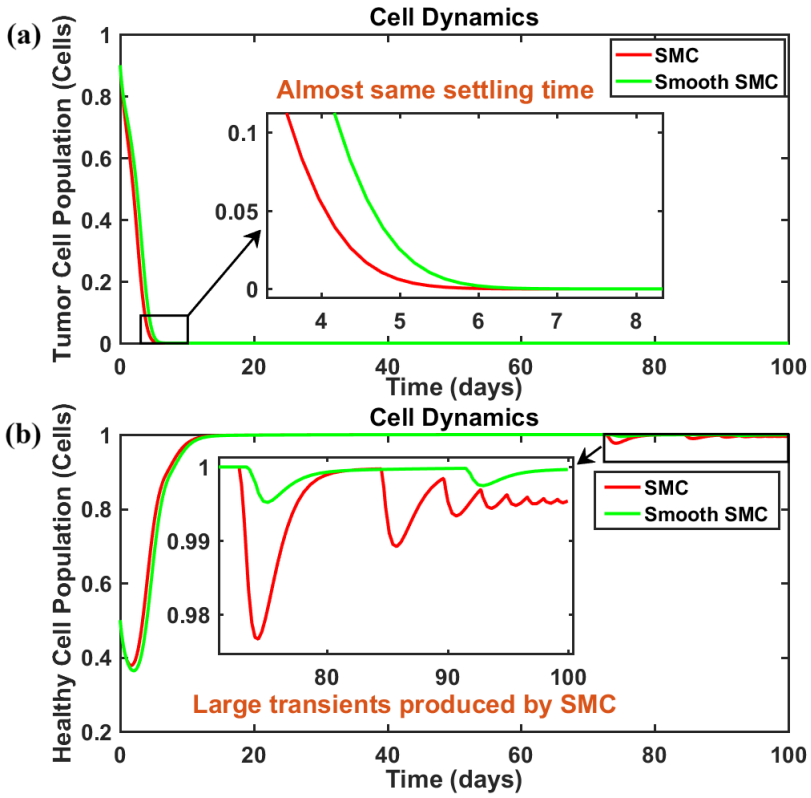

Figure 3. (**a**) Tumor and (**b**) healthy cell dynamics using conventional SMC and proposed smooth SMC.

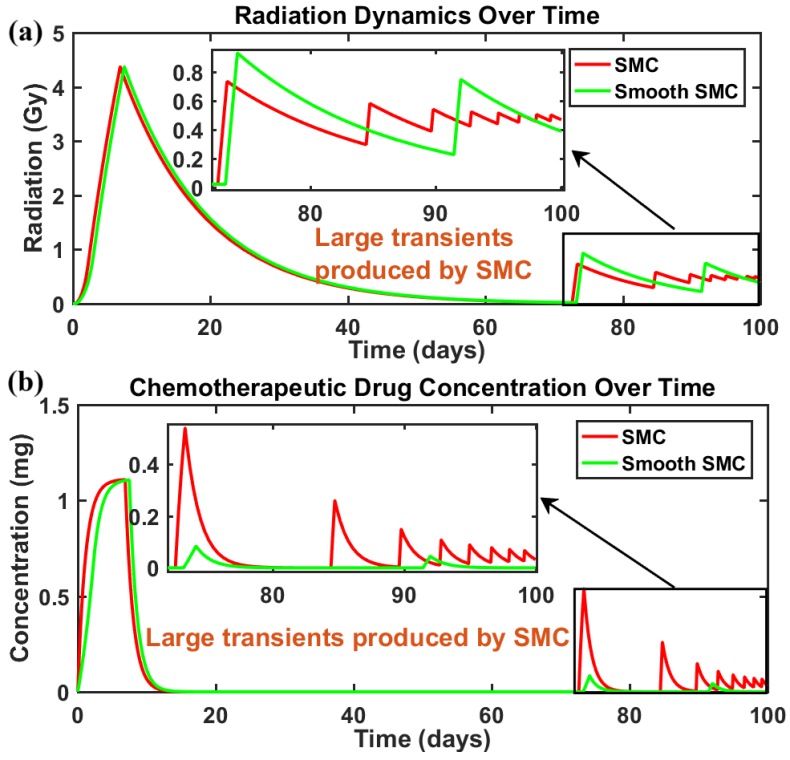

Figure 4. (**a**) Radiation and (**b**) chemotherapeutic drug concentration over time.

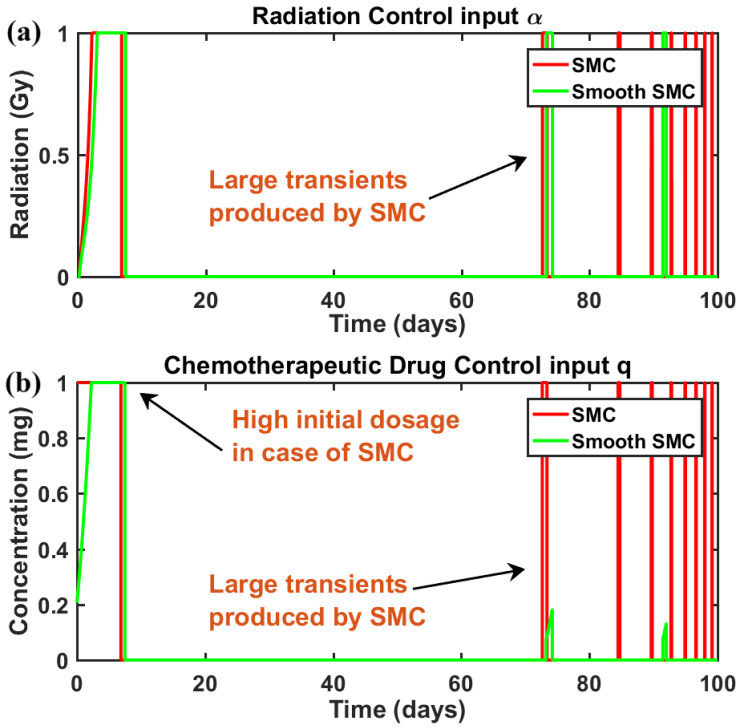

Figure 5. (**a**) Comparison of radiation $\alpha(t)$ and (**b**) chemotherapy $q(t)$ control inputs for conventional SMC and the proposed smooth MISSMC controller.

4.6. Results: Multi-Input Integral Smooth SMC (MIIS-SMC)

The closed-loop responses of tumor and healthy cell populations under conventional (SMC), smooth (MISSMC) and integral smooth SMC (MIIS-SMC) conditions are presented in Figure 6. Figure 6a depicts the dynamics of the tumor cell population, whereas Figure 6b illustrates the dynamics of the healthy cell population. Although all three controllers achieve rapid tumor suppression, the conventional SMC exhibits pronounced transient oscillation in both tumor and healthy cell dynamics due to chattering. The smooth SMC significantly attenuates these oscillations but introduces a small residual steady-state error, as evidenced by the slow decay of the tumor cells within a boundary layer around zero. In contrast, the MIIS-SMC not only preserves the smooth transient behavior but also eliminates the residual steady-state error through integral action. As a result, the tumor population converges asymptotically to zero with improved accuracy, while healthy cells recover faster and remain closer to their desired level with minimal oscillations. This demonstrates that the integral extension effectively compensates for boundary-layer-induced errors without sacrificing smoothness.

Figure 7 illustrates the robustness of the proposed MIIS-SMC under variations in tumor growth rate parameter "r_1", representing tumor heterogeneity and uncertainty. Figure 7a depicts the impact of parameter variation on tumor cell population, whereas Figure 7b illustrates the trajectories of the healthy cell population when the "r_1" parameter is varied. Despite significant changes in r_1, the tumor trajectories consistently converge to zero, while the healthy cell population reliably recovers towards its desired equilibrium. Although parameter variations affect transient behavior, resulting in slightly different tumor decay and healthy cell recovery rates, the steady-state performance remains almost unaffected. This robustness is a direct consequence of the integral action embedded in the sliding surface, which compensates for model mismatch and parameter uncertainty by accumulating and correcting residual tracking errors. These results confirm that the MIIS-SMC framework provides string robustness against biologically realistic parameter variations while maintaining effective tumor mitigation and healthy tissue preservation.

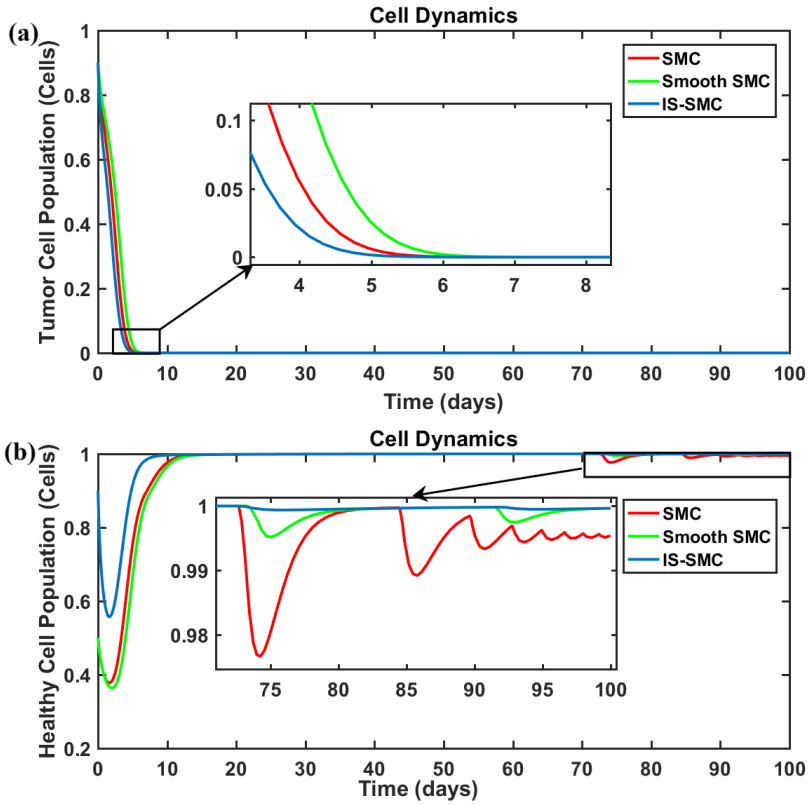

Figure 6. (**a**) Tumor and (**b**) healthy cell dynamics using conventional, smooth and integral smooth SMC.

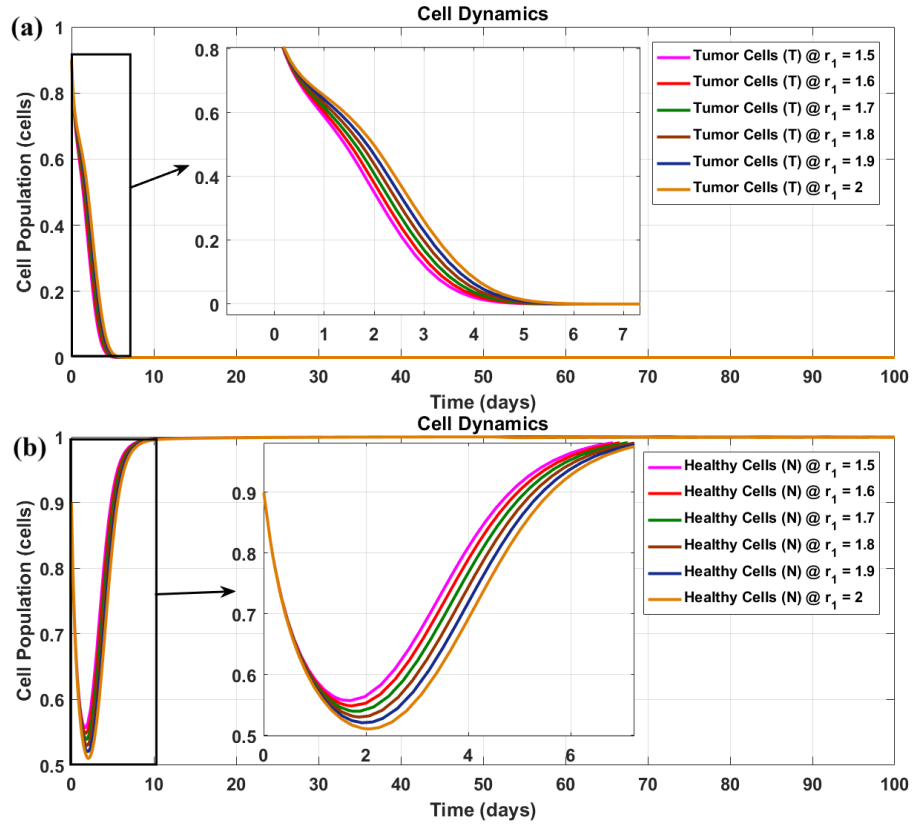

Figure 7. (**a**) Tumor and (**b**) healthy cell dynamics depicting robustness of proposed MIIS-SMC under variations in tumor growth rate parameter "r_1".

4.7. Statistical Analysis

In order to validate the performance of the proposed MISSMC algorithm statistically, four independent Mann–Whitney U tests are performed. The experiment provided in Section 4.5 has been performed repeatedly with slightly modified initial conditions for states "T" and "N" and the results were recorded accordingly. The statistical tests are performed to assess the reduction in transients along with the decrease in overall dosages of administered control inputs by utilizing the proposed MISSMC. The performance data of the proposed controller is recorded in the form of different groups, each containing thirty-two elements. The first two tests compare the total transients observed in the trajectories of control inputs when the proposed MISSMC is employed with those attained by utilizing the conventional SMC. Thus each element in the considered groups represents the total number of observed transients. Similarly, for the next two tests, the total dosages of control inputs administered by the proposed MISSMC are compared with those of the conventional SMC. Thus, for these two tests, each element of the considered groups will represent the amount of administered dosage of control inputs. The outcomes obtained from the statistical tests are subsequently evaluated to substantiate the efficiency, robustness and effectiveness of the proposed MISSMC algorithm in reducing the tumor cell population. Moreover, the analysis will further demonstrate that the algorithm achieves these objectives while consuming lesser amounts of treatment dosages and ensuring smooth administration, thereby mitigating the occurrences of transients.

4.7.1. Test Results—Reduced Transients in α and q

To quantitatively compare the transient behavior produced by the SMC and the proposed MISSMC, the first Mann–Whitney U test depicts a statistically significant reduction in transients in the control input α with the proposed Smooth SMC. A median reduction of 72.7% in transients with a p-value of $1.0142 \times 10^{-12} < 0.05$ indicates that the proposed algorithm significantly reduces the transients in administered radiation control input. Similarly, by utilizing the proposed algorithm, a median reduction of 70% in transients in the chemotherapeutic drug has been observed with a p-value of $1.5663 \times 10^{-13} < 0.05$, indicating that the proposed MISSMC administered the chemo dosages smoothly and thus resulted in significantly reduced transients. A detailed description of the two tests performed along with the raw data is presented in Appendix A.

4.7.2. Test Results—Reduction in Overall Radiation (α) and Chemo Dosages (q)

To quantitatively validate the effectiveness of the proposed MISSMC algorithm in reducing the dosage intensities of both radiation and the chemotherapeutic drug, two Mann–Whitney U tests have been performed by comparing the results of the proposed MISSMC with the conventional SMC. For radiation intensity, by utilizing the proposed algorithm, a median reduction of 0.7% (and mean reduction of 0.7% as well) is observed with a p-value of $3.0487 \times 10^{-5} < 0.05$, implying that the proposed algorithm resulted in a statistically significant reduction in radiation dosage. Similarly, on applying the Mann–Whitney U test to evaluate the reduction in administered chemotherapeutic drug dosage by the proposed algorithm, a p-value of $6.5041 \times 10^{-12} < 0.05$ has been achieved with a median reduction of 26.57% (and mean reduction of 26.7%) in comparison to that of the conventional SMC. A detailed description of these two tests along with the raw data is presented in Appendix B.

5. Discussion: Recently Proposed Algorithms vs. MISSMC

The proposed MISSMC algorithm proved its effectiveness against the tumor cell proliferation in Sections 4.5 and 4.7. Yet, to demonstrate the superiority and efficacy of

the proposed MISSMC algorithm, a comprehensive comparative analysis is conducted in this section. The evaluation assesses the algorithm's abilities and performance both qualitatively and quantitatively, relative to recently developed control strategies.

5.1. Discussion: Qualitative Performance Comparison with Proposed MISSMC and MIIS-SMC

The qualitative performance analysis of the proposed control algorithm is established on the basis of five different criterion. The basis of comparison includes the ability of the feedback controller to administer smooth dosages which result in smooth system dynamics, the types of therapies employed for tumor mitigation, the toxicity-related negative impact on the health of the considered patient, the ability of the controller to converge administered dosages to zero and the settling time (mention as ST) based on the proliferation and growth of healthy and normal cell populations. The qualitative performance parameters of algorithms published in the recent literature are provided in Table 2. Most of the recently proposed algorithms did not evaluate the treatment strategy on the basis of toxicity and procedure-related harmful impacts on human health and general well-being. However, Table 2 provides a comparison of the toxicity caused by the treatment procedure depending on the total dosage required by the respective algorithm to mitigate tumor cell population. In Table 2, N\A stands for not applicable, EH stands for extremely high, VH stands for very high and VL stands for very low, respectively.

Table 2. Qualitative performance comparison with proposed MISSMC and MIIS-SMC.

Source	Smooth Response	Therapy Type	Negative Impact on Health	Input Conv. to 0	ST 2% (Days)
Ref. [30]	×	Chemo	High	✓	10
Ref. [22]	×	Chemo	EH	×	50
Ref. [11]	×	Chemo + Radio	EH	✓	200
Ref. [3]	✓	N\A	N \A	✓	100
Ref. [25] a	×	Chemo	High	✓	60
Ref. [25] b	×	Chemo	High	✓	68
Ref. [25] c	×	Chemo	High	✓	70
Ref. [24]	×	Chemo	High	×	20
Ref. [7]	×	Chemo	High	✓	30
Ref. [2]	✓	Chemo	VH	×	15
Ref. [33]	✓	Chemo + Radio	VL	✓	9
MISSMC	✓	Chemo + Radio	Lowest	✓	11
MIIS-SMC	✓	Chemo + Radio	Lowest	✓	9

Note: ✓ indicates the presence of corresponding feature, while × denotes its absence. Whereas, the Ref. [25] a, b and c denotes synergetic, statefeedback and FLBC algorithms respectively.

Finite-time FLBC has been proposed in Ref. [30] to effectively mitigate tumor proliferation using chemotherapy. Although the controller swiftly subjugated the tumor cell population, it administered a very high dosage of the chemotherapeutic drug to do so, resulting in high levels of toxicity. Moreover, the FLBC algorithm inherently introduced transients in the system dynamics as well. Ref. [22] proposed an optimization-based swarm algorithm to regulate chemotherapeutic drug for tumor mitigation. The algorithm's cost function only considered immediate subjugation of tumor cell population as its only objective, thus resulting in extremely high chemo drug dosages. In a similar fashion, Ref. [11]

proposed an optimal control-based solution utilizing combined radiation and chemotherapy approaches for tumor size reduction. However, the algorithm kept on administering the maximum dosage of radiation and chemotherapeutic drug, even after completely obliterating the tumor. Thus, the algorithm poses severe health risk as it causes extremely high treatment-related toxicity in patients under consideration.

Ref. [3] proposed the combination of backstepping and an SMC-based FLBC algorithm for tumor mitigation. However, the scope of the proposed method is limited, as no treatment procedure is mentioned for the reduction of the tumor. Three nonlinear controllers have been analyzed to regulate chemotherapeutic drug dosage for tumor mitigation in Ref. [25]. In Table 2, Ref. [25] a depicts the performance parameters of the synergetic controller, whereas Ref. [25] b, c mention the performance parameters of statefeedback and FLBC algorithms, respectively. Even though the nonlinear controllers are generally efficient, the proposed algorithms depicted poor performance, sluggish response with transients, and administration of high dosages of chemotherapeutic drug. Another variant of FLBC has been proposed in Ref. [24] that not only suggests to administer high dosages of chemotherapeutic drug for tumor mitigation, but the transient prone control inputs did not converge to zero as well. A similar performance has been achieved using a twin delayed deep deterministic algorithm for tumor mitigation using chemotherapy [7]. The algorithm was able to converge the control input to zero, yet, unlike data-driven reinforcement learning approaches such as TD3, the proposed method provides analytical guarantees on stability, boundedness and dosage limits.

Refs. [2,33] have recently proposed smooth nonlinear control algorithms for the application of tumor mitigation. Ref. [2] suggested the use of a smooth supertwisting algorithm, whereas Ref. [33] proposed a sigmoid function-based smooth synergetic controller. Yet both of them did not explicitly and statistically prove the benefit of employing smoothing functions for transient omission. Similarly, both the proposed MISSMC and MIIS-SMC employed radiation- and chemotherapy-based treatment procedures while administering the least quantities of radiation and chemotherapeutic drug. Thus, the proposed algorithms are least toxic and have the lowest negative impact in comparison to other recently proposed algorithms. Moreover, the proposed MISSMC depicted very swift and robust responses while administering transient-free control inputs, making it very much convenient and risk-free to employ for tumor treatment. Lastly, the proposed MIIS-SMC not only reduced the accumulated steady-state errors, but it also managed to mitigate the impact of parameter mismatch and model uncertainties. Thus following a thorough comparative analysis, it can be concluded that the proposed algorithms demonstrated superior performance compared to recently developed control strategies for tumor mitigation.

5.2. Discussion: Quantitative Performance Comparison with Proposed MISSMC

A detailed quantitative comparison has been established in Table 3 to compare the performance of the recently proposed control algorithms with the novel MISSMC algorithm. This comparison is established on the basis of three comparison parameters. The first parameter is the reduction in baseline control input dosage that a controller administers. The second parameter of comparison is the reduction in tumor mitigation time, i.e., a measure of how fast the proposed MISSMC algorithm subjugated tumor cell population relative to other recently proposed controllers. Lastly, the third parameter of comparison is the reduction in treatment intensity, i.e., a numerical representation of how much reduction in control input dosages occurs when the MISSMC algorithm is employed relative to the other recently proposed controllers.

Table 3. Quantitative performance comparison with proposed MISSMC.

Source	Baseline Dosage Reduction		Faster Tumor Reduction	Treatment Intensity Reduction	
	Chemo	Rad		Chemo	Rad
Optimal-Multi-Input [11]	79%	90%	50%	96.65%	96.51%
Synergetic [25]	79%	–	91.67%	72.25%	–
Statefeedback [1,25]	79%	–	92.65%	55.18%	–
Fuzzy [25,30]	79%	–	92.86%	75.51%	–
PID [25]	79%	–	92.96%	73.04%	–
DRL TD3 [7]	94.17%	–	83.33%	66.24%	–
Supertwisting [2]	79%	–	66.67%	69.45%	–
Sig-Syn [33]	68.65%	76.74	0%	43.07%	43.57%

Most of the algorithms proposed in the recent literature were designed to mitigate tumor cells as swiftly as possible. Thus, these algorithms resulted in administering high initial dosages of control inputs. However, due to the introduction of smoothing functions with conventional control algorithms, the proposed MISSMC resulted in a reduction of initial radiation and chemotherapeutic drug dosages by up to 76.74% and 68.65%, respectively. Similarly, the proposed algorithm effectively relies on both radiation and chemotherapy to not only reduce tumor cell population swiftly but it also contains chemotherapy-related toxicity by relying on radiation therapy. This is evident as the MISSMC reduced the overall dosage requirement of chemotherapeutic drug by up to 43%, whereas the radiation dosage requirement has been reduced by up to 43.57%. However, this reduction in input dosages ended up making the proposed algorithm slightly sluggish in comparison to the smooth sigmoid function-based synergetic controller proposed in Ref. [33], as it converges the tumor population to zero a bit faster. However, the proposed MISSMC still outperforms every other algorithm when compare on the basis of reduction in time taken for tumor mitigation. Algorithms proposed in Refs. [1,2,7,25,30] utilized only a chemotherapy-based approach for tumor mitigation and thus resulted in high baseline as well as overall dosages administered throughout the course of treatment. Thus, the MISSMC algorithm outperforms the recently proposed controllers both qualitatively and quantitatively on the basis of considered parameters.

5.3. Discussion: Challenges and Limitations

The proposed algorithms have demonstrated effectiveness in simulation studies, yet their implementation in practical clinical settings presents several significant challenges and limitations, which are outlined below:

- While the ODE-based model employed in this study is designed to be practical and realistic, it may not cover many aspects of the complex nonlinear nature of real-world biological processes. Many patient-related factors and health conditions significantly influence the tumor's response to combined radiotherapy and chemotherapy. Similarly, tumors themselves exhibit extreme variability in growth, decay, sensitivity and resistance dynamics to different treatment procedures. Hence, a personalized approach that accurately predicts and optimizes based on the tumor's response to therapeutic interventions is more appropriate.
- It is emphasized that the proposed model does not explicitly resolve molecular-scale tumor micro-environment dynamics; instead, these effects are implicitly captured through effective interaction terms, which enables tractable control design and theoretical analysis.

- The performance and effectiveness of recently proposed tumor treatment strategies are dependent on precise and frequent measurements of system states and input dosages. Thus, the practical implementation of these algorithms may require state estimation techniques such as Kalman filtering to compensate for missing or incomplete data and ensure reliable prediction of the system's dynamics.
- In order to practically and clinically utilize the proposed control strategy, strict compliance with safety and efficacy standards from agencies such as the Food and Drug Administration (FDA) or the European Medicines Agency (EMA) is required. Additionally, healthcare professionals would require specialized training to proficiently operate the controller, facilitating a safe and seamless transition from simulation-based studies to real-world clinical application while minimizing potential risks.

5.4. Discussion: Clinical Aspect

The proposed control strategy utilizes the information of system dynamics to compute the radiation and chemotherapeutic drug dosages. All the parameters and states are measured in units per day. This temporal resolution aligns well with the practical feasibility of acquiring state information in clinical settings. In medical practice, key state variables such as tumor size can be reliably obtained though routine laboratory assessments conducted at regular and appropriate intervals. These periodic evaluations support an adequate and realistic estimation of system dynamics, enabling the control algorithm to operate effectively. By adhering to this framework, the proposed approach remains applicable and relevant to real-world scenarios without necessitating continuous or instantaneous state measurements. Recent works including [27,28] illustrate how TME-driven frameworks are increasingly employed to devise synergistic multi-input treatment therapies, including applications beyond oncology. In this perspective, the proposed ODE-based control framework can be interpreted as a high -level decision support and dosage regulation layer that compliments emerging experimental and clinical strategies. This highlights the broader applicability of the proposed control methodology to other diseases and medical conditions where multi-modal interventions are required.

6. Conclusions

This study proposed a rigorous nonlinear control framework for tumor mitigation, based on a multi-input smooth sliding mode control strategy, explicitly incorporating radiotherapy and chemotherapy within a tumor-immune dynamical system. The proposed approach effectively suppresses chattering and large transients by embedding a hyperbolic-tangent function within a sliding manifold. A further integral extension (MIIS-SMC) was introduced to compensate for boundary layer-induced steady-state errors and bounded parameter uncertainties, thereby ensuring asymptotic convergence of tumor and healthy cell states without sacrificing smoothness. From a theoretical standpoint, the closed-loop system was shown to preserve positivity and boundedness, while Lyapunov-based analysis established asymptotic convergence of the sliding surfaces. Explicit upper bounds on radiation and chemotherapy dosages were derived, providing a level of safety assurance that is often absent in control-based tumor treatment studies, thus making the proposed framework particularly attractive for safety-critical biomedical applications. Detailed numerical simulations, supported by statistical analysis, demonstrated that the proposed algorithms substantially reduced transient oscillations in both system states and control inputs when compared to conventional SMC. Furthermore, the results indicate significant reductions in baseline and cumulative treatment dosages, while maintaining effective tumor suppression and healthy cell preservation. Moreover, the proposed MIIS-SMC framework can tolerate biologically realistic parameter variations, such as changes in tumor carrying

capacity, without degradation of steady-state performance. It should be emphasized that the tumor-immune model utilized by this study represents a control-oriented, population-level abstraction rather than a high-fidelity clinical predictor. The radiation-induced tumor mitigation is modeled using a linear term, and treatments are represented as continuous average dose rates. Afterwards, a comprehensive qualitative and quantitative comparison is established between the proposed algorithms and recently proposed controllers to establish their effectiveness and robustness. Overall, the proposed integral smooth sliding mode control framework provides a mathematically rigorous and clinically motivated approach for coordinated radio-chemotherapy design, offering guaranteed stability, reduced toxicity, and improved transient behavior. These features position the method as a promising foundation for future research at the intersection of nonlinear control theory and personalized cancer therapy.

7. Future Research Road-Map

To extend the scope of this research, future investigations will emphasize patient-specific model adaptations by integrating individualized patient data into the mathematical framework to ensure advancements in the development of personalized treatment strategies. Similarly, future work should consider extensions to fractionated or impulsive therapy schedules, incorporation of more detailed radiobiological models (e.g., full linear–quadratic dynamics), and validation against patient-specific or clinical datasets. Integration with data-driven or adaptive schemes could further personalize controller parameters in real-time. Additionally, novel optimization-based algorithms will be incorporated alongside nonlinear control techniques to facilitate a multi-objective approach to simultaneously minimize tumor cell population and treatment-related toxicity while preserving the robustness, smoothness and swiftness of the control algorithm. Furthermore, this optimization framework can be synergized with reinforcement learning-based algorithms, enabling dynamic adjustments to patient-specific parameters based on real-time physiological feedback. By addressing these critical aspects, this research will be extended to bridge the gap between theoretical mathematical modeling and practical clinical applications, ultimately contributing to the development of more effective and personalized cancer treatment protocols.

Author Contributions: Conceptualization, M.A.; methodology, M.A.; software, M.A.; validation, M.A.; formal analysis, M.A.; investigation, M.A.; resources, S.M. and M.T.S.; writing—original draft preparation, M.A.; writing—review and editing, S.M. and M.T.S.; visualization, S.M. and M.T.S.; supervision, S.M. and M.T.S. All authors have read and agreed to the published version of the manuscript.

Funding: This research received no external funding.

Data Availability Statement: The original contributions presented in the study are included in the article. Further inquiries can be directed to the corresponding authors.

Conflicts of Interest: The authors declare no conflicts of interest.

Appendix A

Appendix A.1. Mann–Whitney U Test—Transients in α

The first test compares the performance of the proposed MISSMC with the conventional SMC on the basis of the transients observed in the trajectories of radiation control input α. The first group represents the transients observed in the whole trajectory of the control input α computed by the proposed MISSMC during each experiment with a particular set of initial conditions, whereas group2 contains the total number of transients observed in the computed values of α by the conventional SMC during each experiment at

that same initial conditions corresponding to the group1 elements. Thus, the test is conducted to evaluate which of the two groups achieved tumor suppression more effectively by administering the control input α more smoothly with minimum transients.

group1 = [4, 4, 4, 3, 3, 3, 3, 3, 3, 4, 4, 4, 4, 3, 3, 3, 3, 3, 3, 3, 3, 3, 3, 3, 3, 3, 3, 3, 3, 3] (α: MISSMC)

group2 = [12, 12, 12, 10, 11, 11, 11, 10, 9, 11, 12, 12, 12, 12, 13, 13, 13, 12, 12, 12, 12, 11, 11, 10, 10, 10, 10, 10, 10, 10, 10] (α: conventional SMC)

Considered Null Hypothesis: *There is no significant difference in the observed input transients between the two considered groups.*
Results: The obtained results are as follows:

1. Hypothesis Test Result (h) = 1, which means the null hypothesis is rejected.
2. p-value = $1.0142 \times 10^{-12} < 0.05$.
3. zval = -7.1286: indicates a strong deviation from the considered null hypothesis proving that the MISSMC (group1) produces significantly less transients in comparison to the SMC (group2).
4. ranksum = 528: this also indicates the statistically significant difference between the two groups.

Significance: Statistically, the results signify that the procedure utilized for group1 (MISSMC) results in significantly fewer transients in comparison to the procedure opted for group2 (which utilized conventional SMC).

Appendix A.2. Mann–Whitney U Test—Transients in q

The second test is similar to the first test; however, this time, the basis of comaprison is the chemotherapeutic drug control input q, instead of α. group1 represents the observed transients in q when the proposed MISSMC is utilized, whereas group2 contains the data of observed transients when the conventional SMC was employed.

group1 = [3, 3, 4, 3, 3, 3, 3, 3, 3, 3, 3, 3, 3, 3, 3, 3, 3, 3, 3, 3, 3, 3, 3, 3, 3, 3, 3, 3, 3, 3] (q: MISSMC)

group2 = [11, 11, 11, 9, 10, 10, 10, 10, 9, 10, 11, 11, 11, 11, 12, 12, 12, 11, 11, 11, 11, 10, 10, 10, 10, 10, 10, 10, 10, 10] (q: conventional SMC)

Considered Null Hypothesis: *There is no significant difference in the observed input transients between the two considered groups.*
Results: The obtained results are as follows:

1. Hypothesis Test Result (h) = 1, which means the null hypothesis is rejected.
2. p-value = $1.5663 \times 10^{-13} < 0.05$.
3. zval = -7.3814: indicates a strong deviation from the considered null hypothesis proving that the MISSMC (group1) produces significantly less transients in comparison to the SMC (group2).
4. ranksum = 528: this also indicates the statistically significant difference between the two groups.

Significance: Statistically, the results signify that the procedure utilized for group1 (MISSMC) results in significantly lesser transients in the chemotherapeutic drug control input, in comparison to the procedure opted for group2 (which utilized conventional SMC).

Appendix B

Appendix B.1. Mann–Whitney U Test—Reduction in Overall Radiation Dosage α

This test evaluates the performance of the proposed MISSMC by comparing it to the conventional SMC on the basis of the total radiation dosage administered throughout the course of treatment. Here, group1 represents the total radiation dosage administered during an experiment conducted at a particular set of initial conditions while employing the proposed MISSMC for tumor mitigation. On the other hand, the values of group2 represent the total amount of radiation administered by the conventional SMC for the same particular values of initial conditions as set in corresponding group1 elements. This test is hence conducted to evaluate which of the two groups achieved tumor suppression more effectively by administering the minimum radiation dosage α throughout the treatment procedure.

group1 = [6.8947, 6.9, 6.911, 6.92, 6.923, 6.926, 6.93, 6.934, 6.938, 6.877, 6.86, 6.847, 6.833, 6.82, 6.807, 6.796, 6.784, 6.834, 6.841, 6.85, 6.857, 6.86, 6.87, 6.8755, 6.88, 6.9255, 6.9125, 6.9, 6.89, 6.87, 6.86, 6.8546] (α: MISSMC)

group2 = [6.955, 6.965, 6.977, 6.9533, 6.96, 6.97, 6.976, 6.98, 6.95, 6.936, 6.9182, 6.902, 6.886, 6.872, 6.8764, 6.8743, 6.8623, 6.887, 6.9, 6.913, 6.922, 6.89, 6.905, 6.913, 6.92, 6.95, 6.96, 6.944, 6.932, 6.9065, 6.8992, 6.888] (α: conventional SMC)

Considered Null Hypothesis: *There is no significant difference in the total administered radiation dosage between the two considered groups.*
Results: The obtained results are as follows:

1. Hypothesis Test Result (h) = 1, which means the null hypothesis is rejected.
2. p-value = $3.0487 \times 10^{-5} < 0.05$.
3. zval = -4.1698: indicates a strong deviation from the considered null hypothesis proving that the MISSMC (group1) utilizes statistically and significantly less radiation dosages in comparison to the SMC (group2).
4. ranksum = 729: this also indicates the statistically significant difference between the two groups.

Significance: Hence, the results statistically signify that the proposed MISSMC (group1) results in administration of lower dosage of radiation in comparison to the dose administered by the conventional SMC (group2).

Appendix B.2. Mann–Whitney U Test—Reduction in Overall Radiation Dosage q

This last test is performed to evaluate which of the two considered controllers, i.e., the proposed MISSMC and conventional SMC, administer lesser dosage of chemotherapeutic drug during the whole treatment procedure. The entities of group1 represent the administered chemo dosages throughout an experiment conducted at a particular set of initial conditions. Similarly, the same corresponding initial conditions are utilized to conduct experiments and record administered dosages by employing conventional the SMC in group2. This test is conducted to validate which of the two considered control algorithms administer lesser amounts of chemotherapeutic drug while successfully mitigating the tumor cell population.

group1 = [5.017, 5.2, 5.4, 5.59, 5.8, 6.01, 6.23, 6.46, 6.66, 4.96, 4.912, 4.87, 4.83, 4.795, 4.762, 4.732, 4.704, 4.94, 5.0881, 5.2465, 5.4067, 5.571, 5.74, 5.91, 6.06, 6.51, 6.378, 6.26, 6.15, 5.974,

5.895, 5.823] (q: MISSMC)

group2 = [7.14, 7.3, 7.46, 7.6, 7.76, 7.93, 8.1, 8.27, 8.39, 7.1, 7.063, 7.0312, 7.003, 6.9771, 6.9716, 6.9612, 6.9418, 7.1, 7.23, 7.36, 7.5, 7.6, 7.73, 7.8665, 7.986, 8.3, 8.222, 8.135, 8.057, 7.922, 7.8618, 7.806] (q: conventional SMC)

Considered Null Hypothesis: *There is no significant difference in the total administered chemotherapeutic drug dosages between the two considered groups.*
Results: The obtained results are as follows:

1. Hypothesis Test Result (h) = 1, which means the null hypothesis is rejected.
2. p-value = $6.5041 \times 10^{-12} < 0.05$.
3. zval = -6.8681: indicates a strong deviation from the considered null hypothesis proving that the MISSMC (group1) produces significantly less transients in comparison to the SMC (group2).
4. ranksum = 528: this also indicates the statistically significant difference between the two groups.

Significance: Once again, it is statistically proven that the proposed MISSMC administers significantly lower dosages of chemotherapeutic drug while ensuring efficient and fast tumor mitigation.

References

1. Zubair, M.; Ahmad, I.; Islam, Y.; Islam, A. Lyapunov based nonlinear controllers for the chemotherapy of brain tumor. *Biomed. Signal Process. Control* **2021**, *68*, 102804. [CrossRef]
2. Rsetam, K.; Al-Rawi, M.; Cao, Z.; Alsadoon, A.; Wang, L. Model based smooth super-twisting control of cancer chemotherapy treatment. *Comput. Biol. Med.* **2024**, *169*, 107957. [CrossRef]
3. Sarhaddi, M.; Yaghoobi, M. A new approach in cancer treatment regimen using adaptive fuzzy back-stepping sliding mode control and tumor-immunity fractional order model. *Biocybern. Biomed. Eng.* **2020**, *40*, 1654–1665. [CrossRef]
4. American Cancer Society. *Survival Rates for Bladder Cancer*; American Cancer Society: Atlanta, GA, USA, 2024.
5. Tang, Y.; Su, H.; Jin, T.; Flesch, R.C.C. Adaptive PID Control Approach Considering Simulated Annealing Algorithm for Thermal Damage of Brain Tumor During Magnetic Hyperthermia. *IEEE Trans. Instrum. Meas.* **2023**, *72*, 4002108. [CrossRef]
6. Angom, R.S.; Nakka, N.M.R.; Bhattacharya, S. Advances in Glioblastoma Therapy: An Update on Current Approaches. *Brain Sci.* **2023**, *13*, 1536. [CrossRef] [PubMed]
7. Hoda, M.; Mostafa, N.; Fatemeh, J.; Meskin, N. Deep reinforcement learning-based control of chemo-drug dose in cancer treatment. *Comput. Methods Programs Biomed.* **2024**, *243*, 107884. [CrossRef]
8. Dixon, M.; Phan, T.A.; Dallon, J.; Tian, J.P. Mathematical model for IL-2-based cancer immunotherapy. *Math. Biosci.* **2024**, *372*, 109187. [CrossRef]
9. Gaiaschi, L.; Bottone, M.G.; Luca, F.D. Towards Effective Treatment of Glioblastoma: The Role of Combination Therapies and the Potential of Phytotherapy and Micotherapy. *Curr. Issues Mol. Biol.* **2024**, *46*, 14324–14350. [CrossRef]
10. Stupp, R.; Mason, W.P.; Bent, M.J.V.D.; Weller, M.; Fisher, B.; Taphoorn, M.J.B.; Belanger, K.; Brandes, A.A.; Marosi, C.; Bogdahn, U.; et al. Radiotherapy plus Concomitant and Adjuvant Temozolomide for Glioblastoma. *N. Engl. J. Med.* **2005**, *352*, 987–996. [CrossRef]
11. Kumar, A.; Dubey, U.S.; Dubey, B. The impact of radio-chemotherapy on tumour cells interaction with optimal control and sensitivity analysis. *Math. Biosci.* **2024**, *369*, 109146. [CrossRef] [PubMed]
12. Duwe, G.; Knitter, S.; Pesthy, S.; Beierle, A.S.; Bahra, M.; Schmelzle, M.; Schmuck, R.; Lohneis, P.; Raschzok, N.; Öllinger, R.; et al. Hepatotoxicity following systemic therapy for colorectal liver metastases and the impact of chemotherapy-associated liver injury on outcomes after curative liver resection. *Eur. J. Surg. Oncol.* **2017**, *43*, 1668–1681. [CrossRef]
13. Anton, S.C.; Santamaria, G.M.; Garcia, A.M.; Redondo, M.G.A. State of the art in melanoma brain metastatic treatment and evidence of combined high-dose radiotherapy and immunotherapy approach. *Adv. Radiother. Nucl. Med.* **2024**, *2*, 3499. [CrossRef]
14. Alghamdi, M.; Bazarbashi, S.; Mahrous, M.; Alshaer, O.; Gad, A.M.; Aseafan, M.; Abdelgelil, M.; Alshabi, R.M.; Alghanmi, H.A.; Naser, N.A.; et al. Outcomes of Patients with Metastatic Colorectal Cancer Treated with Trifluridine/Tipiracil beyond the Second Line: A Multicenter Retrospective Study from Saudi Arabia. *J. Oncol.* **2022**, *2022*, 3796783. [CrossRef]

15. Yazdjerdi, P.; Meskin, N.; Al-Naemi, M.; Mostafa, A.E.A.; Kovacs, L. Reinforcement learning-based control of tumor growth under anti-angiogenic therapy. *Comput. Methods Programs Biomed.* **2019**, *173*, 15–26. [CrossRef]
16. Gonzalez-Crespo, I.; Gomez-Caamano, A.; Pouso, O.L.; Fenwick, J.D.; Pardo-Montero, J. A Biomathematical Model of Tumor Response to Radioimmunotherapy With alpha-PDL1 and alpha-CTLA4. *IEEE/ACM Trans. Comput. Biol. Bioinform.* **2023**, *20*, 808–821. [CrossRef]
17. Davis, A.; Gao, R.; Navin, N. Tumor evolution: Linear, branching, neutral or punctuated? *Biochim. Biophys. Acta (BBA) Rev. Cancer* **2017**, *1867*, 151–161. [CrossRef] [PubMed]
18. Zhang, R.; Wang, T.; Shen, H.; Zhou, X.; Han, Q.; Li, L.; Zhang, L.; Wang, C.; Dong, X. Tumor Microenvironment-Responsive MnOx-Mesoporous Carbon Nanoparticles for Enhanced Chemodynamic Synergistic Antitumor Therapy. *ACS Appl. Nano Mater.* **2025**, *8*, 2763–2773. [CrossRef]
19. Procopio, A.; Cesarelli, G.; Donisi, L.; Merola, A.; Amato, F.; Cosentino, C. Combined mechanistic modeling and machine-learning approaches in systems biology—A systematic literature review. *Comput. Methods Programs Biomed.* **2023**, *240*, 107681. [CrossRef] [PubMed]
20. Sharifi, N.; Ozgoli, S.; Ramezani, A. Multiple model predictive control for optimal drug administration of mixed immunotherapy and chemotherapy of tumours. *Comput. Methods Programs Biomed.* **2017**, *144*, 13–19. [CrossRef] [PubMed]
21. Patmanidis, S.; Charalampidis, A.C.; Kordonis, I.; Mitsis, G.D.; Papavassilopoulos, G.P. Tumor growth modeling: Parameter estimation with Maximum Likelihood methods. *Comput. Methods Programs Biomed.* **2018**, *160*, 1–10. [CrossRef]
22. Shindi, O.; Kanesan, J.; Kendall, G.; Ramanathan, A. The combined effect of optimal control and swarm intelligence on optimization of cancer chemotherapy. *Comput. Methods Programs Biomed.* **2020**, *189*, 105327. [CrossRef]
23. Wu, X.; Hou, Y.; Zhang, K. Switched system optimal control approach for drug administration in cancer chemotherapy. *Biomed. Signal Process. Control* **2022**, *75*, 103575. [CrossRef]
24. Ay, S.; Soylu, S. Optimal fuzzy P + D controller for cancer chemotherapy. *Biomed. Signal Process. Control* **2024**, *96*, 106634. [CrossRef]
25. Qaiser, H.; Ahmad, I.; Kashif, M. Fuzzy, synergetic and non-linear state feedback control of chemotherapy drug for a cancerous tumor. *Biomed. Signal Process. Control* **2020**, *62*, 102061. [CrossRef]
26. Khalili, P.; Vatankhah, R. Optimal control design for drug delivery of immunotherapy in chemoimmunotherapy treatment. *Comput. Methods Programs Biomed.* **2023**, *229*, 107248. [CrossRef]
27. Wang, Y.; Xu, Y.; Song, J.; Liu, X.; Liu, S.; Yang, N.; Wang, L.; Liu, Y.; Zhao, Y.; Zhou, W.; et al. Tumor Cell-Targeting and Tumor Microenvironment-Responsive Nanoplatforms for the Multimodal Imaging-Guided Photodynamic/Photothermal/Chemodynamic Treatment of Cervical Cancer. *Int. J. Nanomed.* **2024**, *19*, 5837–5858. [CrossRef]
28. Yang, J.; Zhu, J.; Lu, S.; Qin, H.; Zhou, W. Transdermal psoriasis treatment inspired by tumor microenvironment-mediated immunomodulation and advanced by exosomal engineering. *J. Control. Release* **2025**, *382*, 113664. [CrossRef] [PubMed]
29. Özgür Doruk, R. Angiogenic inhibition therapy, a sliding mode control adventure. *Comput. Methods Programs Biomed.* **2020**, *190*, 105358. [CrossRef]
30. Dhanalakshmi, P.; Senpagam, S.; Mohanapriya, R. Finite-time fuzzy reliable controller design for fractional-order tumor system under chemotherapy. *Fuzzy Sets Syst.* **2022**, *432*, 168–181. [CrossRef]
31. Zubair, M.; Rana, I.A.; Islam, Y.; Khan, S.A. Variable Structure Based Control for the Chemotherapy of Brain Tumor. *IEEE Access* **2021**, *9*, 107333–107346. [CrossRef]
32. Jiao, H.; Shen, Q.; Shi, Y.; Shi, P. Adaptive Tracking Control for Uncertain Cancer-Tumor-Immune Systems. *IEEE/ACM Trans. Comput. Biol. Bioinform.* **2021**, *18*, 2753–2758. [CrossRef]
33. Arsalan, M.; Yu, X.; Sadiq, M.T.; Almogren, A. Simultaneous Multi-Treatment Strategy for Brain Tumor Reduction via Nonlinear Control. *Brain Sci.* **2025**, *15*, 207. [CrossRef]
34. Mohite, U.L.; Patel, H.G. Optimization assisted Kalman filter for cancer chemotherapy dosage estimation. *Artif. Intell. Med.* **2021**, *119*, 102152. [CrossRef] [PubMed]
35. Chen, L.; Zhang, Y.W.; Zhang, S.C. Optimal Drug Dosage Control Strategy of Immune Systems Using Reinforcement Learning. *IEEE Access* **2023**, *11*, 1269–1279. [CrossRef]
36. Arora, G.; Bairagi, N.; Chatterjee, S. A mathematical model to study low-dose metronomic scheduling for chemotherapy. *Math. Biosci.* **2024**, *372*, 109186. [CrossRef] [PubMed]
37. Kuznetsov, V.A.; Makalkin, I.A.; Taylor, M.A.; Perelson, A.S. Nonlinear dynamics of immunogenic tumors: Parameter estimation and global bifurcation analysis. *Bull. Math. Biol.* **1994**, *56*, 295–321. [CrossRef]
38. de Pillis, L.G.; Radunskaya, A.E.; Wiseman, C.L. A Validated Mathematical Model of Cell-Mediated Immune Response to Tumor Growth. *Cancer Res.* **2005**, *65*, 7950–7958. [CrossRef]

39. Urszula, L.; Heinz, S. Antiangiogenic Therapy in Cancer Treatment as an Optimal Control Problem. *SIAM J. Control Optim.* **2007**, *46*, 1052–1079. [CrossRef]
40. Hamza, A.; Ahmed, I.; Uneeb, M. Fuzzy logic and Lyapunov-based non-linear controllers for HCV infection. *IET Syst. Biol.* **2021**, *15*, 53–71. [CrossRef]